POLITECNICO DI MILANO

Facoltà di Ingegneria Industriale e dell'Informazione

Corso di Laurea Magistrale in Ingegneria Biomedica

Biomechanical modeling of Femoropopliteal artery

Modello biomeccanico dell'arteria Femoro-Poplitea

Supervisor: Professor

Francesco Migliavacca

Co - supervisor:

Dr. Michele Conti

Dr. Alexey Kamenskiy

Author:

Giulia Campanile

UIN **824100**

Academic year 2015/2016

Alla mia famiglia

Acknowledgments

First of all I would like to thanks Dr. Michele Conti because, once again, he supported me, helped me a lot and gave me this great opportunity to work on this interesting project that permits me also to spend a period abroad, an amazing experience.

I express ma sincere thanks to Professor Migliavacca for let me undertake this work of thesis.

I'm very thankful to Dr. Kamenskiy and Dr. MacTaggart for invited me to spend this outstanding month at UNMC in Omaha, where i learned a lot, as an engineer, as a student but moreover as a person, thank you for making this possible.

I'm very grateful to have met and worked with all this amazing group, thank you very much Anastasia, Paul, William, Silvye and Eric for being so nice with me, including me in your team since the first day, I will never forget it.

Summary

Background and aims

Endovascular devices implanted in the femoropopliteal artery (FPA) are exposed to a unique set of mechanical loadings due to the proximity of the artery with the knee joint. The assessment of such loadings, related to the arterial kinematics, and their impact on both the long-term clinical outcomes and device failure [1] are certainly a relevant scientific topic for both biomechanical and vascular surgery community [2]. In fact, several studies, ranging from analytical modeling of FPA deformation [3] to the complete numerical 3D patient-specific modeling of the thigh/artery/joint system [4], are already available in literature. Unfortunately, such approaches are often cumbersome and difficult to tailor to patient-specific characteristics. Moved by these considerations, the present study proposes a computational model based on structural finite element analysis (FEA) aimed at understanding the complex biomechanical behavior of the FPA.

Materials and methods

The model is implemented in Abaqus/STD (Simulia, Dassault Systèmes, Providence, RI, USA) and the input file for the non-linear finite-strain FEA is created by a Matlab script (MathWorks, Natick, Mass). As depicted in Figure 1, the following main parts define the model:

- FPA: a portion of the SFA and the popliteal artery is modelled as a beam (el. Type B21) with a constant circular section with a diameter of 8mm. Arterial tissue is modelled as linear elastic material ($E = 2MPa, \nu = 0.33$).

- Bones and leg boundaries: two rigid beams represent the femur and tibia respectively. Two additional beams are positioned posteriorly, behind the artery, to resemble the boundary of the thigh and the calf. Bone tissue is modeled as linear elastic material ($E = 18GPa, \nu = 0.2$).

- Tissue/muscles surrounding the artery: they are modeled with spring elements; these elements, evenly spaced, connect the artery with the surrounding parts. *SpringA* elements of Abaqus library are adopted, i.e., axial spring between two nodes, whose line of action is the line joining the two nodes. This line of action may rotate in large-displacement analysis.

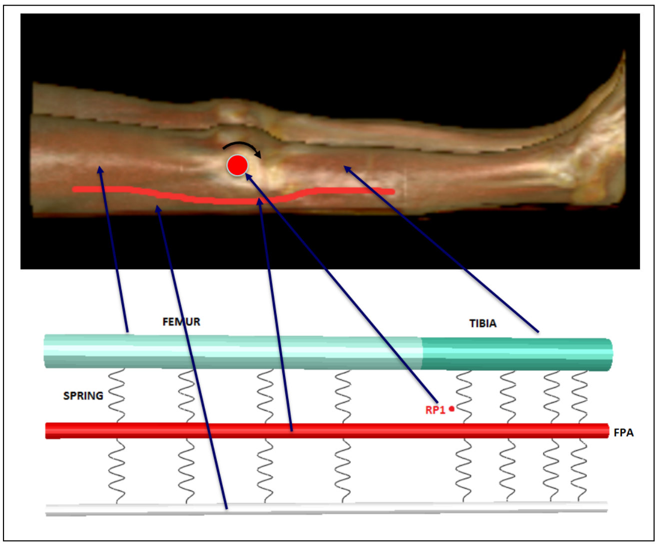

Figure 1: Schematic representation of the femoropopliteal artery modeling.

The analysis is composed by two steps: we first simulate the arterial prestretch and its dependence to the age, accounting for the indications reported by Kamenskiy et al. (2016) [5]; then, we simulate the knee bending as detailed in the following. The deformation of the artery due to leg flexion is induced by the rotation of the tibia model around a reference point (RP) corresponding to the knee joint, where a given angle of rotation is enforced as a boundary condition. A multipoint constraint – *MPC* - type *BEAM* is used to connect the RP and the tibia model. A given, consistent displacement is imposed to the arterial ends. The total number of nodes is less than 1000, so the simulation can be performed by Abaqus 6.14 Student Edition and run on a standard laptop (Processor 2,9 GHz Intel Core i7) in less than one minute.
Three main types have been performed with an increasing level of complexity: 1) 2D idealized model; 2) 2D patient-specific model; 3) 3D patient-specific model.

Results and conclusions

This section illustrates simulation results which are principally related to the 2D idealized model; some preliminary results related to 2D patient-specific model and the 3D one are also presented. in Figure 2 we have the undeformed model and the vessel prestretched, then we see the result of the FE analysis of a 90° and a 110° knee flexion. Outcomes suggest that the model is able to capture the main features of the femoropopliteal biomechanics during the knee bending, nevertheless is simplicity. We decide to evaluate the outcomes of the model following two different methods

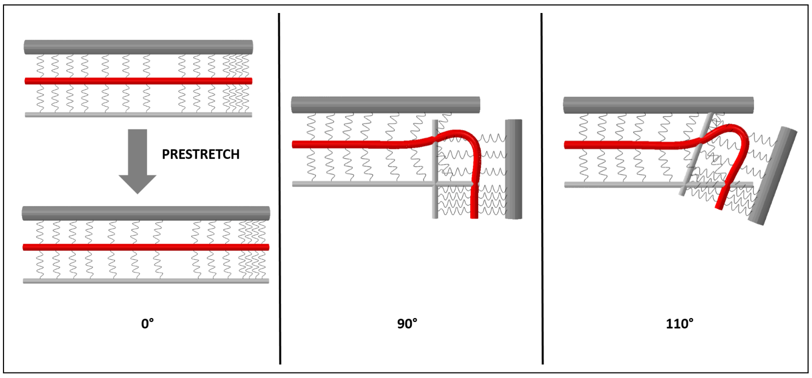

Figure 2: Results of the analysis. From the left: undeformed vessel and vessel prestretched, 90° knee flexion simulation, 110° knee flexion simulation.

detailed below: evaluating arterial deformations increasing age, in relation with prestretch; and we study the vessel behavior stiffening a portion of the artery part, modeling a stent.

Ageing and prestretch

We evaluate relationship that prestretch, as a function of age [5], has with the length surplus of the artery, first indication of tortuosity. The length surplus as suggested by Wensing et al. (1995) [3] is the ratio between the arterial length after the knee bending and its potential shortest path. Then we study the relationship with curvature along the length of the artery itself. The outcomes, showed in Figure 3, agreeing with literature's indications, say that with ageing the length surplus increases because the artery is less able to accomodate shortening existing during knee flexion, and so the curvature's values, with higher peaks above the knee where the FPA physiologically is more free to move.

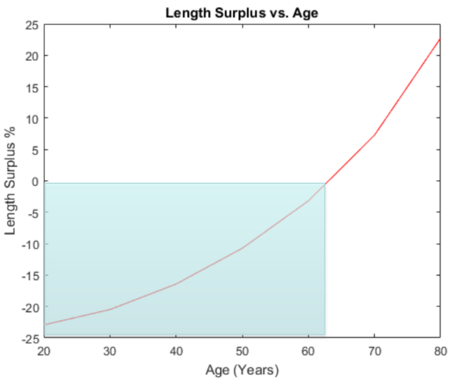

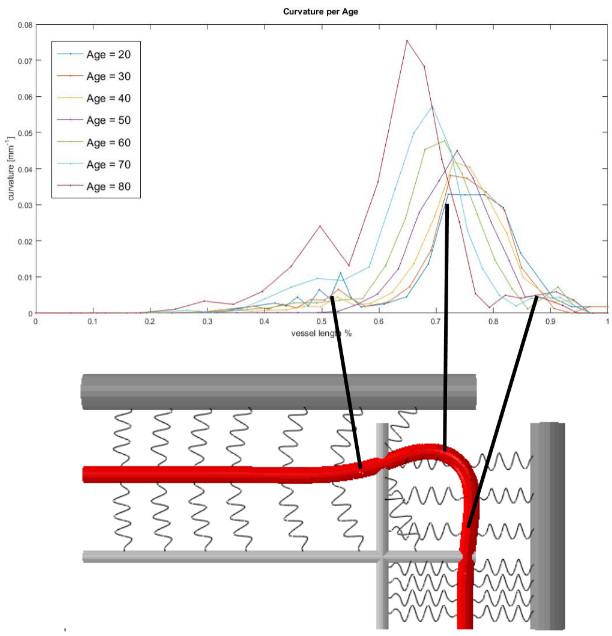

Figure 3: Results of an increasing of age. On the left: Length Surplus VS Age. On the right: Curvature per Age.

Regional stiffening: stent

Then we study the behavior of FPA during knee flexion increasing the Young modulus in a region of the vessel part, trying to evaluate arterial/stent interaction. Even in this case results agree with literature. Length surplus decreases, with the increasing of stiffness, because vessel can bend less, getting less tortuous. Curvature in the stiffer portion decreases as well, increasing instead dramatically at the edge of stented region, resulting in sharp kinks, evaluated in literature as the main cause of stent failure and fracture. We see these outcomes in Figure 4.

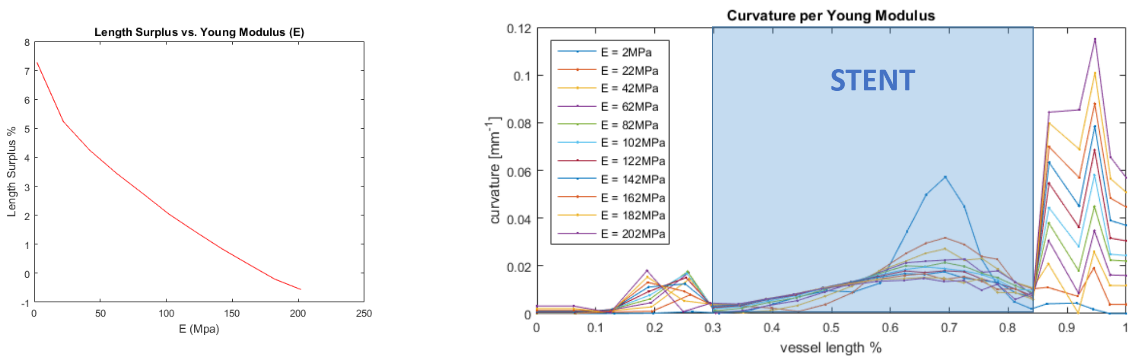

Figure 4: Results of a regional stiffening modeling a stent. On the left: Length surplus VS Young modulus. On the right: Curvature per Young modulus. The stiffer region is higlighted in blue.

Patient specific models

From the analysis of the second 2D model, in Figure 5 we show how interesting is the result in bending adding the coordinates of the centerline and diameters of the patient's vessel.

Despite the main limitation of a two dimensional environment, that make us loosing some

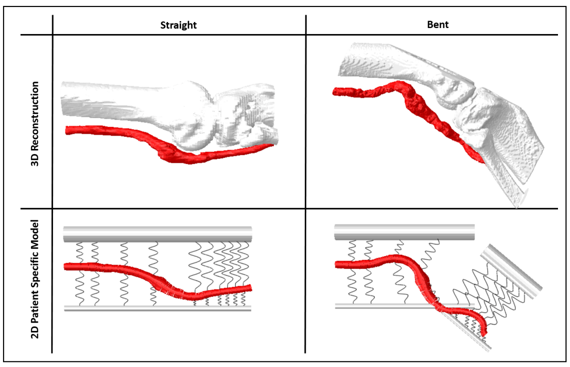

Figure 5: Patient CT scans reconstruction (at the top), FE model (at the bottom). In the left column we have the straight leg, in the right column we have the leg and the model after 40° knee flexion.

important information, these two models, with a very low computational cost, permit to catch the general behavior of the region. In the third model we try to overcome this limitation and the preliminary results are very promising, an example in Figure 6.

The final aim of this project is to further refine the models, in particular the patient-specific ones,

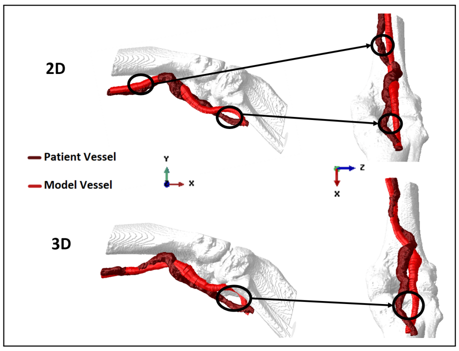

Figure 6: Preliminary results of 3D model compared to the previous 2D one.

and validate it, to predict the impact of stenting, with respect to patient-specific data extracted by in-vivo images or ex-vivo experiments, like the ones performed by Dr. Kamenskiy and his group of research at University of Nebraska Medical Center, with whom we collaborate thanks to this project of thesis.

References

[1] Petrini, L., Trotta, A., Dordoni, E., Migliavacca, F., Dubini, G., Lawford, P. V., and Pennati, G. (2015). A Computational Approach for the Prediction of Fatigue Behaviour in Peripheral Stents: Application to a Clinical Case. Annals of biomedical engineering, 1-12.

[2] Kamenskiy, A., Nusz, S., Hunter, W., Desyatova, A., Ruhlman, M., Pipinos, I., and MacTaggart, J. (2015). Effects of Demographics and Clinical Risk Factors on Human Femoropopliteal Artery Histopathology. Arteriosclerosis, Thrombosis, and Vascular Biology, 35(Suppl 1), A713-A713.

[3] Wensing, P. J., Scholten, F. G., Buijs, P. C., Hartkamp, M. J., Mali, W. P., and Hillen, B. (1995). Arterial tortuosity in the femoropopliteal region during knee flexion: a magnetic resonance angiographic study. Journal of anatomy, 187(Pt 1), 133.

[4] Ghriallais, R. N., and Bruzzi, M. (2014). A computational analysis of the deformation of the femoropopliteal artery with stenting. Journal of biomechanical engineering, 136(7), 071003.

[5] Kamenskiy, A., A. Seas, G. Bowen, P. Deegan, A. Desyatova, N. Bohlim, W. Poulson, and J. Mac-Taggart (2016). In situ longitudinal pre-stretch in the human femoropopliteal artery. Acta Biomaterialia 32, 231-237.

[6] Conti M., Marconi M., Campanile G, Reali A., Adami D., Berchiolli R., Auricchio F. Patient-specific finite element analysis of popliteal stenting. Meccanica. DOI: 10.1007/s11012-016-0452-9

Sommario

Introduzione

I dispositivi endovascolari impiantati nell'arteria femoro-poplitea (FPA) sono sottoposti a sollecitazioni uniche dovute alla vicinanza dell'arteria all'articolazione del ginocchio. La valutazione di questi particolari carichi, legati alla cinematica del vaso, il loro impatto sui risultati clinici ed il fallimento degli stent [1] sono certamente argomento di importanza scientifica rilevante sia per la biomeccanica che per la chirurgia vascolare [2]. Numerosi studi sono presenti in letteratura, a partire dalla valutazione delle deformazioni della FPA [3] fino ad arrivare a modelli numerici 3D paziente-specifici del sistema gamba/arteria/articolazione [4]. Molto spesso però la complessità di questi modelli è troppo elevata ed è inoltre difficile adattarli ai dati dello specifico paziente. Spinti da queste osservazioni presentiamo, in questo studio, un modello computazionale basato su un'analisi agli elementi finiti (FEA) per comprendere meglio il comportamento biomeccanico della FPA.

Materiali e metodi

Il modello è implementato in Abaqus/STD (Simulia, Dassault Systèmes, Providence, RI, USA) e l'input file per la FEA non lineare in grandi deformazioni è creato da uno script Matlab (MathWorks, Natick, Mass). Come vediamo nella Figura 1, le parti seguenti definiscono il modello:

- FPA: una porzione dell'arteria Femorale Superficiale (SFA) e l'arteria Poplitea sono modellizzate da travi (elementi B21) con una sezione circolare costante pari a 8mm. Il comportamento maccanico del tessuto arterioso è stato riprodotto con un materiale elastico lineare ($E = 2MPa,\ \nu = 0.33$)

- Ossa e contorni anatomici della gamba: due travi rigide rappresentano il femore e la tibia. Due ulteriori travi sono posizionate dietro l'arteria, riproducono il contorno anatomico di coscia e polpaccio. A queste parti è stato assegnato un materiale elastico lineare ($E =$

18GPa, $\nu = 0.2$)

- Tessuti e muscoli circostanti l'arteria: simulati da molle che collegano il vaso alle altre parti. Sono utilizzati elementi *SpringA* della libreria di Abaqus, ovvero molle assiali tra due nodi, in cui la linea d'azione è la congiungente tra i due nodi. Questa linea d'azione può ruotare in condizioni di grandi spostamenti.

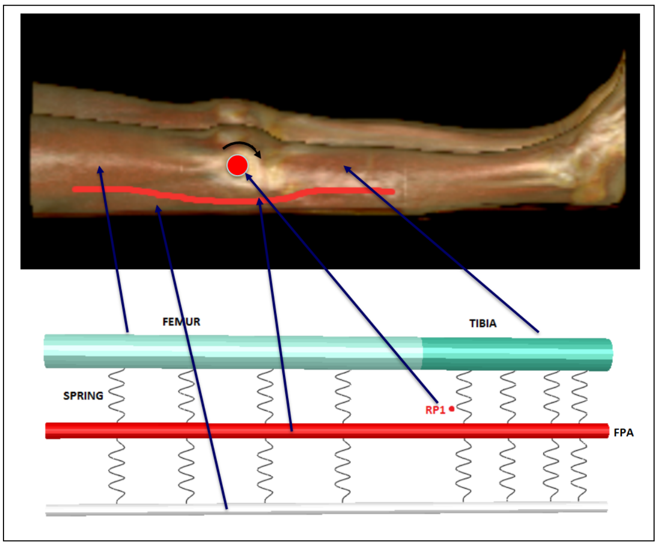

Figure 1: Rappresentazione schematica del modello dell'arteria femoro-poplitea.

L'analisi comprende due fasi; nel primo implementiamo il prestretch dell'arteria seguendo le indicazioni fornite da Kamenskiy et al. (2016) [5] sulla relazione con l'età del paziente; nel secondo simuliamo la flessione della gamba. La deformazione del vaso è indotta dalla rotazione della tibia intorno ad un *reference point* corrispondente all'articolazione del ginocchio, sul quale è definito un angolo di rotazione come condizione al contorno. Un *multipoint constraint* - *MPC* - di tipo *BEAM* viene utilizzato per vincolare il *reference point* alla tibia. Imponiamo quindi al vaso un consistente spostamento. Il numero totale dei nodi nel modello è inferiore a 1000, di conseguenza la simulazione può essere effettuata nella Student Edition di Abaqus 6.14 ed è possibile eseguirla su un computer standard (Processore 2.9 GHz Intel Core i7) in meno di un minuto. Abbiamo sviluppato tre diverse tipologie di modello con una specificità crescente: 1) un modello 2D idealizzato; 2) un modello 2D paziente specifico; 3) un modello 3D paziente specifico.

Risultati e conclusioni

In questa sezione illustriamo i risultati delle simulazione principalmente relativi al modello idealizzato 2D; sono riportati inoltre alcuni risultati preliminari connessi ai modelli 2D e 3D paziente specifici. Nella Figura 2 vediamo il modello all'istante iniziale e dopo il prestretch; inoltre mostriamo il risultato di due diverse analisi, una con una rotazione del ginocchio di 90° e l'altra di 110°. I risultati mostrano come l'analisi sia in grado di cogliere le caratteristiche principali della biomeccanica dell'arteria durante il piegamento del ginocchio, nonostante la sua semplicità.

Successivamente elencheremo i risultati estratti seguendo due differenti metodi di valutazione:

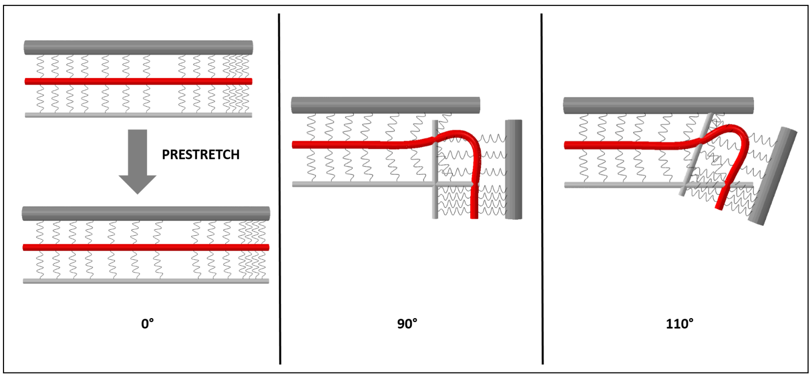

Figure 2: Risultato delle analisi. Da sinistra: vaso indeformato e vaso dopo il prestretch, simulazione di piegamento del ginocchio a 90°, simulazione di piegamento del ginocchio a 110°.

nel primo definiamo la relazione tra l'età, e conseguente prestretch, e le deformazioni del vaso; nel secondo simuliamo, tramite un irrigidimento locale del vaso, l'applicazione di uno stent, e ne valutiamo il comportamento.

Età e prestretch

Valutiamo come il prestretch, funzione dell'età [5], sia legato al *length surplus* dell'arteria, come prima indicazione della tortuosità. Il *length surplus* è definito da Wensing et al. (1995) [3] come il rapporto tra la lunghezza del vaso e il suo percorso più breve. Successivamente abbiamo studiato la relazione del prestretch con la curvatura lungo l'arteria. I risultati, riportati in Figura 3, in accordo con la letteratura, evidenziano come al crescere dell'età il *length surplus* aumenti, in quanto l'arteria è sempre meno in grado di accomodare gli accorciamenti esistenti durante la flessione della gamba, e così anche i valori di curvatura, che mostrano picchi in prossimità del ginocchio, dove l'arteria è, anche anatomicamente, meno vincolata.

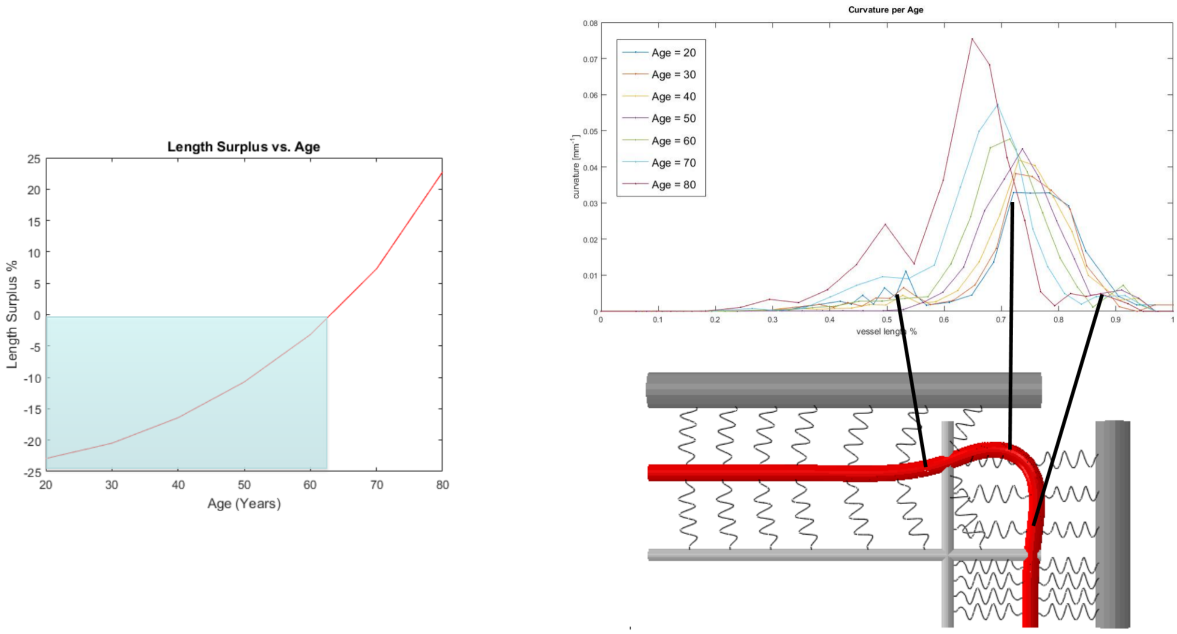

Figure 3: Risultati dell'aumento dell'età. Sulla sinistra: *length surplus* rispetto all'età. Sulla destra: valori di curvatura all'aumentare degli anni.

Irrigidimento localizzato e simulazione impianto di stent

Successivamente abbiamo studiato il comportamento del nostro modello di FPA durante la flessione del ginocchio aumentando gradualmente il modulo di Young in una porzione del vaso, cercando così di stimare le interazioni arteria-stent. Anche in questo secondo caso ci siamo trovati in accordo con la letteratura esistente. Il *length surplus* diminuisce, all'aumentare della rigidezza locale, infatti ora il vaso può deformarsi meno diventando meno tortuoso. La curvatura decresce nella regione più rigida, ma sottolineiamo come agli estremi di questa regione aumenti sensibilmente, con la formazione di piegamenti molto pronunciati che sono annoverati in letteratura come tra le principali cause di rottura e fallimento dello stent. In Figura 4 illustriamo i risultati.

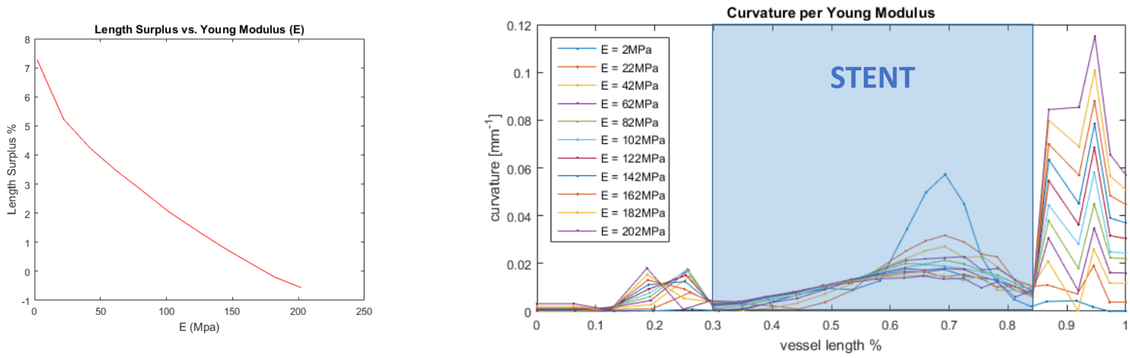

Figure 4: Risultati dell'irrigidimento locale. A sinistra: *length surplus* rispetto al modulo di Young (E). A destra: andamento della curvatura all'aumentare di E. Evidenziamo inoltre in blu la regione di irrigidimento locale.

Modelli paziente specifici

Dalle analisi effettuate sul secondo modello 2D, in Figura 5, vediamo quanto interessante sia il risultato ottenuto aggiungendo la centerline e i diametri reali dell'arteria del paziente. Nonostante

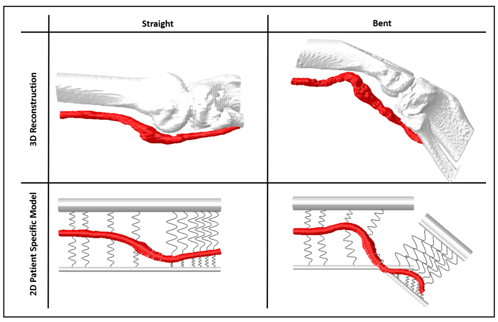

Figure 5: Ricostruzione di immagini TC del paziente (in alto), modello FE (in basso). A sinistra abbiamo la gamba distesa, a destra la gamba piegata di un angolo di 40°.

la maggior limitazione dell'utilizzo di un ambiente 2D, che può comportare una forte perdita di informazioni, questi due modelli, con un costo computazionale decisamente basso, permettono di cogliere il comportamento generale di questa regione. Nel terzo modello cerchiamo di superare questo limite e i primi risultati estratti sono promettenti. Un esempio in Figura 6.

Come obiettivo finale di questo studio ci poniamo di perfezionare i modelli, specialmente i

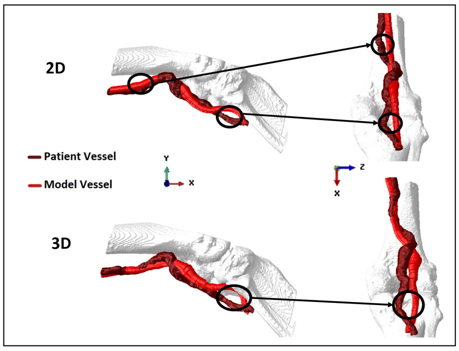

Figure 6: Risultati preliminari del modello 3D paragonato al precedente modello 2D.

casi paziente-specifici, così da poter predire l'impatto dello stent [6], con una validazione sui dati estratti da pazienti o esperimenti ex-vivo, come quelli effettuati dal Dr. Kamenskiy e il suo gruppo di ricerca del Medical Center dell'Università del Nebraska con il quale abbiamo collaborato grazie a questa attività di tesi.

Riferimenti bibliografici

[1] Petrini, L., Trotta, A., Dordoni, E., Migliavacca, F., Dubini, G., Lawford, P. V., and Pennati, G. (2015). A Computational Approach for the Prediction of Fatigue Behaviour in Peripheral Stents: Application to a Clinical Case. Annals of biomedical engineering, 1-12.

[2] Kamenskiy, A., Nusz, S., Hunter, W., Desyatova, A., Ruhlman, M., Pipinos, I., and MacTaggart, J. (2015). Effects of Demographics and Clinical Risk Factors on Human Femoropopliteal Artery Histopathology. Arteriosclerosis, Thrombosis, and Vascular Biology, 35(Suppl 1), A713-A713.

[3] Wensing, P. J., Scholten, F. G., Buijs, P. C., Hartkamp, M. J., Mali, W. P., and Hillen, B. (1995). Arterial tortuosity in the femoropopliteal region during knee flexion: a magnetic resonance angiographic study. Journal of anatomy, 187(Pt 1), 133.

[4] Ghriallais, R. N., and Bruzzi, M. (2014). A computational analysis of the deformation of the femoropopliteal artery with stenting. Journal of biomechanical engineering, 136(7), 071003.

[5] Kamenskiy, A., A. Seas, G. Bowen, P. Deegan, A. Desyatova, N. Bohlim, W. Poulson, and J. Mac-Taggart (2016). In situ longitudinal pre-stretch in the human femoropopliteal artery. Acta Biomaterialia 32, 231-237.

[6] Conti M., Marconi M., Campanile G, Reali A., Adami D., Berchiolli R., Auricchio F. Patient-specific finite element analysis of popliteal stenting. Meccanica. DOI: 10.1007/s11012-016-0452-9

Contents

List of Figures

Chapter 1

Background and aims

Peripheral arterial disease (PAD) comprises those entities which result in obstruction to blood flow in the arteries, exclusive of the coronary and intracranial vessels (Ouriel, 2001). In particular the incidence of PAD in the lower extremities is quite high and treatment not so efficient, so far. In this work of thesis we concentrate our efforts in understand the complex biomechanics of the femoropopliteal artery (FPA), that is the main vessel of the lower limb and one of the major in the human body, connecting the iliac artery to the tibial bifurcation. This complex local behavior, especially in the popliteal segment right above the knee, is the main reason of treatment's failure that often leads to an amputation of the leg below the knee.
This chapter starts with a brief overview of the anatomical features of the FPA discussing also the main pathologies and the corresponding therapeutic procedures. Finally, the goal of the thesis and its organization is presented.

1.1 Anatomy of the the Femoral artery and Popliteal artery

The femoral artery is the terminal branch of the external iliac artery; it is the most important vessel, about the arterial circuit, of the inferior art. It begins behind the inguinal ligament, between the lacuna of the vessels and ends in the channel of the adductor muscles. After that area it takes the name of popliteal artery. It goes down in the antero-medial region of the thigh. At the beginning it occupies the lateral angle of the lacuna of the vessels, just behind the inguinal ligament. It is also in front of the insertion of the pectineus muscle. It is divided in two branches, the superior one, called as femoral branch and the interior called genito-femoral. It passes also throw the Scarpa triangle in its first part. Out of the triangle it goes behind the sartorial muscle. The femoral vein is placed just below the artery. As introduced just above, below the articulation of the knee, there is the poplipeal artery. It goes from the adductor channel to the arch tendon of the soleus muscle. Over this point it branches into two vessels called the tibial anterior and the tibial posterior artery (Schuenke et al., 2010). In Figure 1.1 these regions are showed. In this area the course of the vessel is quite straight and there are not much branches. However the incidence of vascular pathologies is, as mentioned above, quite relevant; this point means that the mechanical factors are very important to be understood. The pathologies in this area are very frequents; however also the possibilities of treatment; in the next section there would be reported some of them.

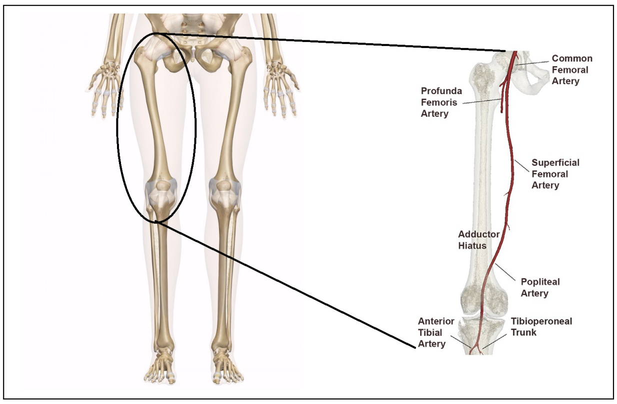

Figure 1.1: Anatomy of the femoropopliteal artery. Figure adapted from the work of MacTaggart et al. (2014).

1.2 Femoropopliteal diseases

Peripheral arterial disease is considered to be a set of chronic or acute syndromes, generally derived from the presence of occlusive arterial disease, which causes inadequate blood flow to the limbs. From the pathophysiologic point of view, ischemia of the lower limbs can be classified as functional or critical. Functional ischemia occurs when the blood flow is normal at rest but insufficient during exercise, presenting clinically as intermittent claudication. Critical ischemia is produced when the reduction in blood flow results in a perfusion deficit at rest and is defined by the presence of pain at rest or trophic lesions in the legs. In this situation, precise diagnosis is fundamental, as there exists a clear risk of loss of the limb if adequate blood flow is not re-established, either by surgery or by endovascular therapy, (Hernando and Conejero, 2007).
PAD are greatly correlated with age and many risk factors are connected with these pathologies such as diabetes, hypertension, smoking, and hyperlipidemia as in cerebrovascular and heart ischemic disease, (Norgren et al., 2007). One difference between PAD of lower limb and pathologies of coronary and cerebral arteries is the composition of the plaque, femoropopliteal's plaques are very stenotic and fibrous, while coronary's are more lipidic covered by a thin fibrous layer more susceptible to rupture, (Hernando and Conejero, 2007). In Figure 1.2 we can see an example of stenosis due to atherosclerosis, i.e., deposition of plaques. It is usually possible to evaluate the degree of stenosis with the help of imaging techniques, such as MRI or CT, or with the Ankle

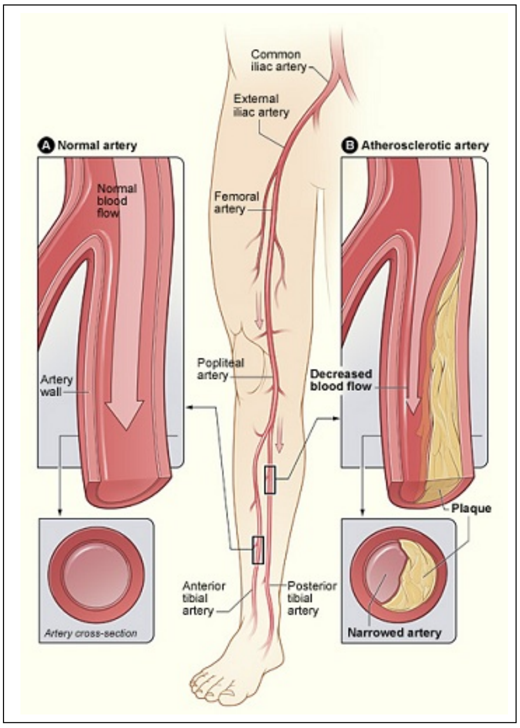

Figure 1.2: Representation of stenosis examples that affect the femoral artery, (National Insitute of Health, 2015).

Brachial Index (ABI) defined as the rate between the blood pressure in the ankle and the blood pressure in the upper arm, An ABI between and including 0.9 and 1.2 is considered normal (free from significant PAD), while a lesser than 0.9 indicates arterial disease (Collaboration, 2008). These methods permit to decide which is the best intervention to perform for the health of the patient. The degree of stenosis is measured as the percentage of the narrowing of the radius of the vessel compared to its normal measure.

Another important e quite frequent pathology of this region is the aneurysm. Aneurysmal disease in FPA is defined as a focal or fusiform dilation 1.5 times the normal diameter and it's related to disruption, fragmentation and altered balance in the mechanical integrity of the arterial wall (Hurks et al., 2014). Aneurysmal disease can lead to distal ischemia, i.e., lack of bloodflow to the limb, due to embolization or thrombosis, mass or blood clot that can travel in the bloodstream and occlude the vessel, and rarely rupture. Even aneurysm can be diagnosticated with medical imaging such as MRI or CT and Doppler ecograph, to evaluate speed and direction of blood flow. These pathologies can be caused by the complex kinematics of this vessel, and by the strong external solicitation force acting here, these same issues have been classified as the ones that provoke failures in treatments of this region.

1.3 Treatments

Obviously the first therapy is the reduction of risk factor and lifestyle modification; but, when the phase of the pathology is too advanced two are the types of treatment used so far: open surgical intervention or endovascular intervention.

1.3.1 Open surgical intervention

Untill today the gold standard for treatments in case of severe PAD in the FPA is the bypass. Bypass graft is connected above and below the vessel blockage and the blood is rerouted through the graft, as in Figure 1.3. They can be autogenous such as the greater saphenous vein, small

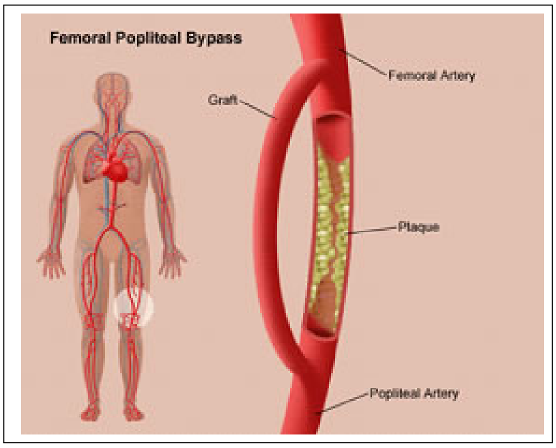

Figure 1.3: Representation of femoral bypass.

saphenous vein, superficial femoral vein, criopreserved vein and radial artery, or prosthetic using Dacron, PTFE e ePTFE, (Mills, 2016).
Autogenous are normally cosidered more durable, when there is no available vein in below the knee bypass PTFE is the more used.

1.3.2 Endovascular interventions

In this case we have Angioplasty, with the use of balloons inserted to open the occluded vessel, but patency rate after few years decreases dramatically; atherectomy that is a minimally invasive tecnique for physically removing atherosclerosis from vessels' wall, but the plaques remained could disturb the bloodflow causing other pathologies and fast re-occlusion. The most promising technique is the use of stent, covered with ePTFE membrane or uncovered, generally, in this region, nitinol memory foam self expanding devices Figure 1.4.

As less invasive, endovascular interventions, especially stents, should be the more preferable treatments for vascular diseases. Unfortunately surrounding structures and tissues have a large impact on the FPA, this artery is unique in that it is a long muscular artery, traversing a long

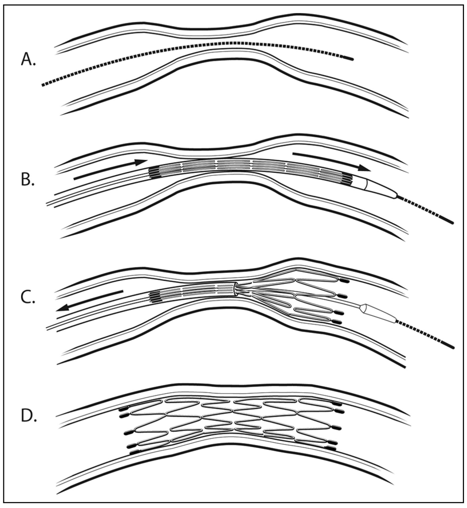

Figure 1.4: The steps of a self expanding stent deploying procedure: (A) a steerable wire is softly advanced across the stenotic lesion; (B) the undeployed stent is delivered to the target; (C) the stent is deployed; (D) final result.

distance and is surrounded by multiple muscle groups. Kinematic movement and limb deformations produce arterial deformation and unique stresses and strains and high degree of tortuosity; these are the reasons why stent devices often fail and why there's the need to improve the design.

1.4 Goals of the work and its organization

The main goal of the thesis is simulating the kinematics behavior of the vessel through the creation of a fast, immediate but reliable FE model. The organization of the chapters of this work is the following:

- 2- Literature Review → to introduce the reader to the topic, the first paragraph after the introduction is dedicated to the literature review of the works regarding popliteal kinematics or in general aspects of the popliteal artery. We consider only works published in the last twenty years;
- 3- 2D Model → this chapter is the core of all the thesis project, we present our 2D general model with results, discussion and limitations, base of all the subsequent work and future developments.
- 4- Patient Specific Model → Here we present the patient specific version of the model in 2 dimensions and 3 dimensions.
- 5- About internship at UNMC → This chapter deals with the description of my experience at University of Nebraska Medical Center in Omaha, where, above all, I could assist to a

cadaver's dissection in order to get some important data for validating the model in the future works.

- 6- Conclusions and future work

At the end of all this chapter the reader will understand completely the procedure we propose.

Chapter 2

Literature review

From an engineering point of view studying the biomechanics of femoropopliteal artery and consequent stents failure has been translated in mathematical model for the quantification of vessel deformation or computational finite element analysis model (FEA). Different data have been taken for each of these studies and different methods have been used, in this chapter we try to highlight the major contributes present in literature dividing them in three main sections the first for medical image analysis, the second for experimental analysis and the third for FEA modeling.

2.1 Medical image analysis

Wensing 1995

The article, written by Wensing et al. (1995), is probably the first work regarding the analysis of the kinematics of the superficial femoral artery (SFA) during the bending of the knee. The study is conduced on a group of 22 people of different ages, between 23 and 68 years old; both males and females. Magnetic resonance angiography (MRI) is the technique of images performed on the patients. Wensing and Scholten create for the first time a 2D model of the SFA configuration during bending, as depicted in Figure 2.1. They deeply investigate with a series of geometric calculations, not reported here, the strong changing in configuration of this vessel during bent leg. What they find is that there is a length excess in the vessel during the flexion. This excess is corrected with 2 physiological techniques: the compensation made, that ends with the S shape configuration and the elasticity of the vessel. From the measure of the radius R of the curve in sagittal plane of the S, they get with some steps an estimation of the arterial elasticity. The main interest of the authors is to investigate the way in which the femoral artery copes with length excess as a result of knee flexion. The main conclusions of this study are the following: i) they understand that vessel tortuosity developing during the knee flexion is age dependent. Besides, S angle decreases with age due to the stiffness increase of the vessel; ii) the tortuosity is mainly caused by elasticity, that has a strong negative correlation with age, that means that the vessel accommodates less the shortening, bending more sharply.

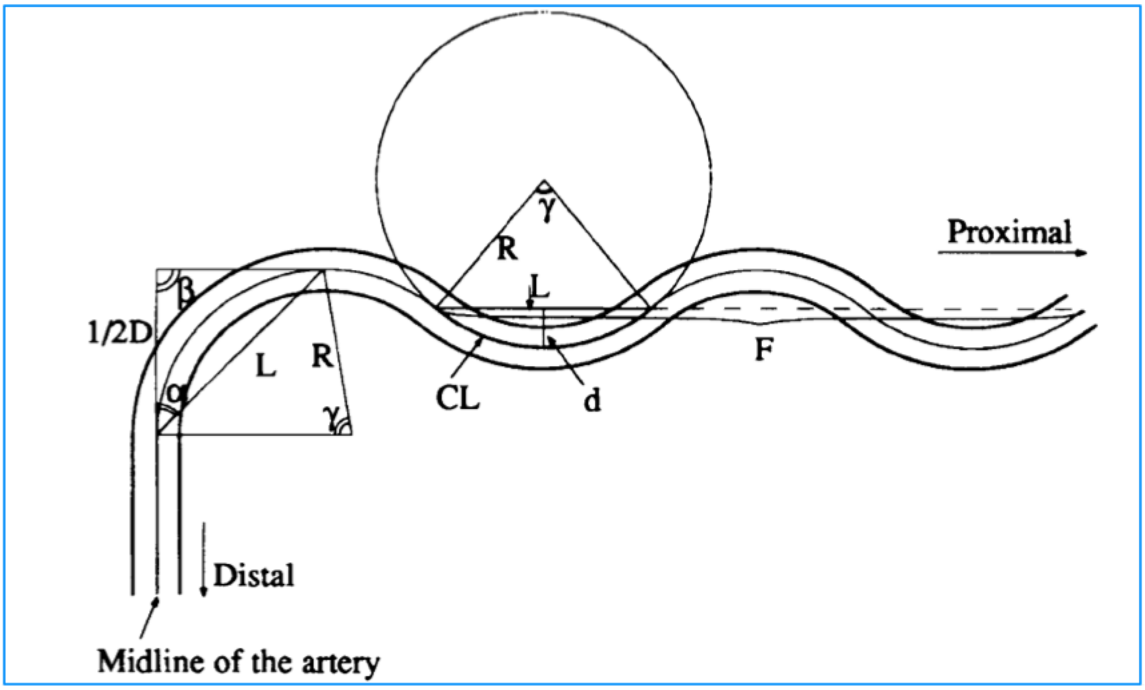

Figure 2.1: Wensing's model showing the first model in literature than tries to explain the kinematics of the poplitea in the case of 90° of the knee.

Cheng 2006

To quantify in vivo deformations of the superficial femoral artery of young people, during maximum knee and hip flexion, that they propose as the goal of their study, Cheng et al. (2006) use as technique of imaging a common MRI machine. They measure SFA fetal length, supine length and angle of twist, as shown in Figure 2.2. All the measures are made both for the left and the right vessel, with the purpose to understand if there was any intra-patient difference. From the last measurement they finally understand that the transition from supine to fetal position causes a significant SFA twisting that could give rise to several future problems for the stenting. Furthermore the vessel in fetal position results more compressed than in all other positions. This compression is probably a great cause of stent fracture. The last important result that this team find is that SFA deformation cannot be assumed similar in different people; in other words it is not possible to assume similarity intra-people.

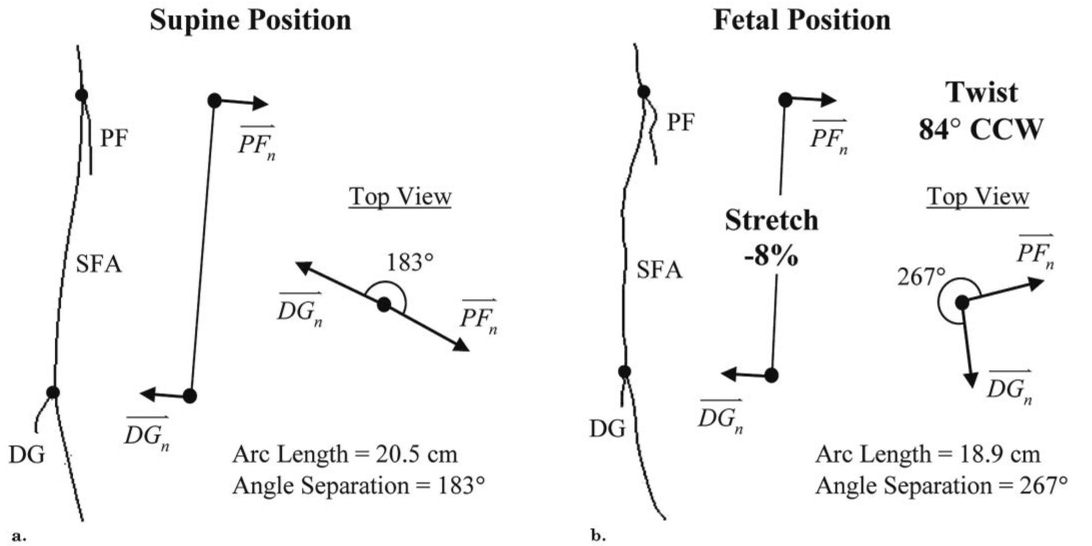

Figure 2.2: Calculation of SFA axial stretch and angle of twist in a representative left leg.

Choi 2009

The next work that appears in the literature through the years is the article of Choi et al. (2009). In this paper, the first thing that comes clear as a strange fact to the eye of the reader is that the age of the eight volunteers, that is not coherent with the profile of a person who usually needs a SFA/popliteal stent implantation (20-36 years old), as we previous saw with the article described in the section above of Cheng et al. Anywhere, differently to the other work that appears in this literature review chapter, that focus their attention specifically on SFA and popliteal artery, the goal of this work is not to analyze specific solution for a femoral stent but in general to aid the developing of more durable endovascular devices; including stent and stent grafts. All the images have been taken with both MRA and Computed Tomography. With the first, the team take the principal images of the area, with the second method they make the measurements, after the elaboration of the images taken. Without taking into account the other anatomical areas that they investigate, about the superior femoral artery (SFA), they measure the shortening of it, comparing the length between supine position and bent leg, simulating sitting position. Another information that they get is the maximum curvature of the vessel.
As a result they notice that their method is valid for a lot of different types of vessels and they also are able to quantify deformations in examples of different various vessels, such as abdominal aorta, common iliac artery, SFA and LAD.

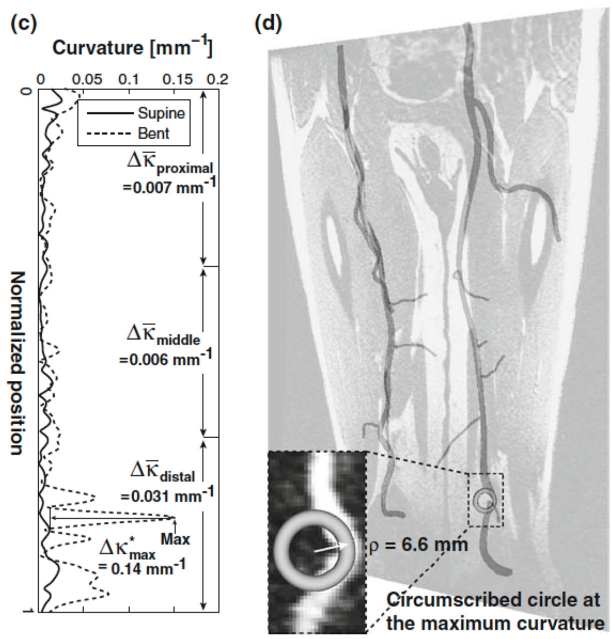

Figure 2.3: The analysis of the variation of the curvature down to the superficial femoral artery, comparing the values of straight leg and bent one.

Cheng 2010

As we saw until now about literature the work made by Cheng et al. (2010) is very innovative if compared to the others. For the first time the investigation is made considering only the most probable patients, according to the age, that could need a SFA stent implantation. However, also here images are taken from 7 healthy volunteers with MRI. The main goal of this job is to describe geometric changes of the superficial femoral artery (SFA) resulting from hip and knee flexion, expressly in old people. To reach this point Cheng and his team make a series of measurements, concentrating on the shortening. After that they measure also the deformations of the third and bottom part of the SFA and they notice that there, the deformation and the curvature are more significant than in the other two areas. The cause is probably the less musculoskeletal constraint in that area compared to the one in others.

Ganguly 2011

Ganguly et al. (2011) concentrate as the other the analysis into old patients. In particular, the volunteers are aged 67. The technique of analysis in different in comparing to other works; indeed Ganguly, instead of what others author used MRA, decides to use computed tomography (CT). However, this is not the unique innovation of this work. For the first time somebody studies what happen during the bending of the knee with the presence of a stent, in the femoral artery, into an alive patient. The main limit of this work is that the stents are not the same in sizes and lengths and, in many cases, multiple stents from different manufacturers were implanted during their treatment. It is not yet immediate to compare the results of different samples.

They evaluate the stent length compression during bending, the stent curvature and they get as a result that chronic fatigue is still the main cause of stent fracture.

2.2 Experimental analysis

Smouse 2005

Smouse et al. (2005) make a great step forward with respect to Wensing et al. (1995). They choose as case of study cadavers. The number of patient in their study is not so high, only 7 people. However, they make an intelligent choice: they decide to analyze both legs to discover if there is any intra-patient difference, and also to have more available data. They use angiography, for getting more detailed images of the vessels. They introduce for the first time the stent into the vessel during the analysis in order to study its interaction. They perform the measurements simulating two different situation: the walking one and the sitting position, evaluating deformations such as shortening and bending angle, and at the end axial rigidity of the vessel. From the evaluation of results comes out that for the stented artery the shortening is lower, and between stented artery is higher for shorter stents. Furthermore, with longer and more rigid stents, the ability of the artery to axial compression is severely compromised. Once axial compression is maximized, the entire arterial segment bends or undulates to accommodate the shorter distance between the hip and the calf. They even discover that the bending is the main cause of stent fracture at least concerning the ones they investigated. Another problem is shown in the left subfigure below depicted in Figure 2.4 adjacent stents separated by bare artery may shift out of the plane during joint bending.

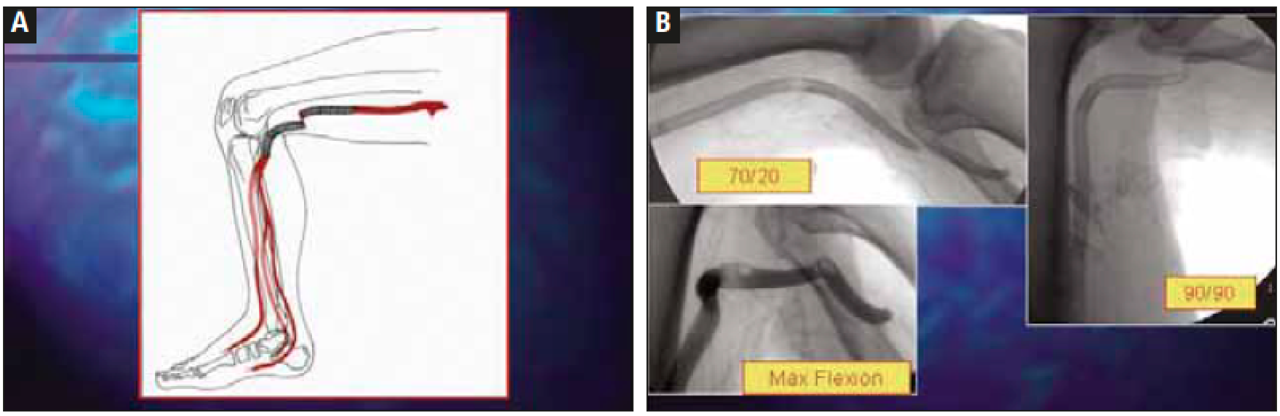

Figure 2.4: Left figure: a realistic simulation of the configuration of the vessel during knee bending. Right one: the MRA images of what effectively happen into the vessel.

Nikanorov 2009

This is the second of three works made from the collaboration between Alexander Nikanorov (2009) and Doctor Smouse. This work have 2 main purposes: to characterize the types and ranges of stent distortion theoretically produced by extremity movement, and as second one to use these ranges as parameters for in vitro long-term fatigue testing of commercially available self-expanding nitinol stents. Also in this case cadavers are used for the study. The idea is to measure the shortening and the bending in degrees of the stent and use them for in vitro fatigue testing. 5 commercial self expanding stents are used. The main result is the comparison between value of compression and distortion of unstented arteries and stented ones. The results are reported below in the table, the angles are about the bending of the knee and the hip. The first line corresponds to the value of shortening in case of unstented artery, the second line in case of stented one.

90°/90° Bending		
Popliteal Artery	Middle SFA	Distal SFA
14%	9%	23%
11%	3%	6%

To make this analysis more real, because as we said before they work with cadavers, phosphate - buffered saline (37±2°) was circulated through the closed system for all the duration of the experiment, to reproduce natural conditions into the vessels. As it is easy to read from this table the results are that nitinol self-expanding stents undergo both axial and bending deformation when implanted into the superficial femoral, middle and distal, and popliteal arteries. Furthermore, commercially available stents exhibit a variable ability to withstand chronic deformation in vitro, and their response is highly dependent on the type of deformation applied. As conclusion of this paragraph we reported here below, in Figure 2.5 the comparison in length found with the bending of the knee in the vessel. In the figure are also reported the exact measures found with the MRI.

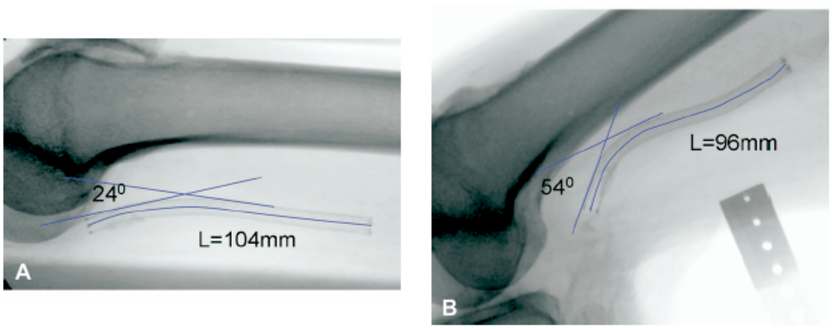

Figure 2.5: Evaluation of the popliteal stent length in case of straight leg (A) and bent leg (B).

Kamenskiy 2014

One improvement in study of SFA biomechanics has been done from the research group of Dr. Kamenskiy from University of Nebraska Medical Center (UNMC), MacTaggart et al. (2014). In this work they invent an interesting way to measure arterial deformation on 5 lightly embalmed cadavers. They use a fishing line with several markers attached on it, as shown in Figure 2.6, and they deploy it in the femoropopliteal artery of the cadaver. They find smart ways to measure bending, torsion and axial compression from the cadaver's leg CT scan in straight and different bending position, finding that they are higher than previously reported. The limitations of this work is the use of lightly embalmed cadavers, because is still unknown how closely they match the in vivo arterial characteristics, that may affect deformation measurements, though it seems to resemble the elasticity of the artery of diabetic patients. But the measurements taken can definitely help to evaluate the mechanical environment of FPA in order to improve tratments and reconstruction of this vessel.

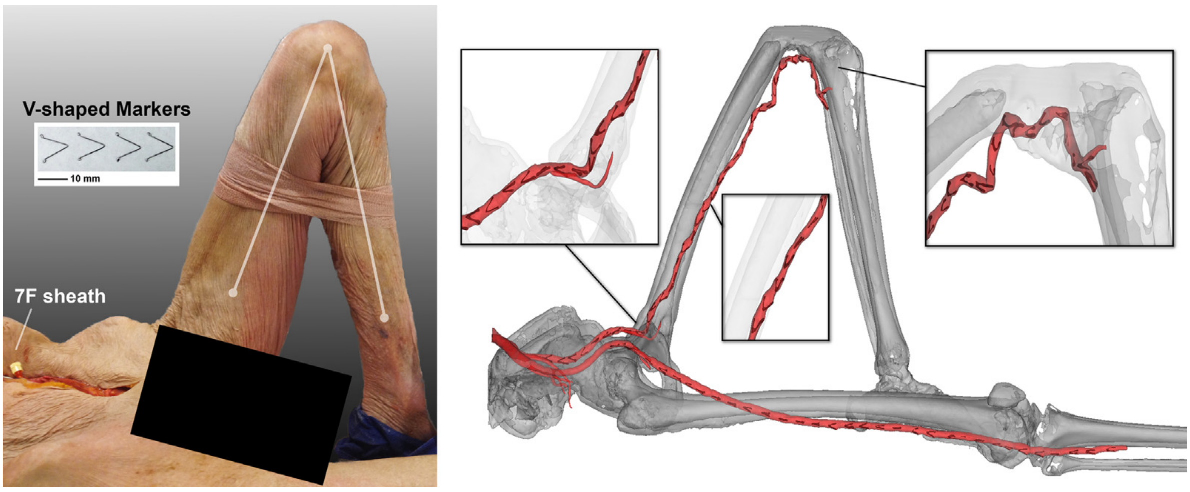

Figure 2.6: Left: V-shaped markers deployed endovascularly into the limb of a lightly embalmed cadaver through the sheath placed in the abdominal aortic bifurcation; right: 3D reconstruction of the CT scan of the same cadaver with inserts demonstrating magnified views of the proximal SFA, mid SFA and below knee PA regions in the straight and acutely bent limb. The knee joint in the right panel of the figure is not visualized because it was outside of the CT scanner field of view.

2.3 Computational models

Diehm 2011

Diehm et al. (2011) purpose is to predict within a certain accuracy the deformation of femoropopliteal artery using FEA model based on real patients MRI but without patient specific material properties and without detailed muscles modeling. They use MRI with contrast media bolus of 8 healthy patients in straight and bent (40°) leg position, they reconstruct 3D model of bones and soft tissues, included artery and they implement a FEA imposing 40° rotation of the tibia to the femur. Comparing centerline of MRI and FEA vessel of bent leg, as we can see in Figure 2.7 they find that motions predicted were similar in all of the cases except for two, the two tallest patient with low body mass index. The two main issues of this study were the bending of only 40° and the high assumption of modeling artery and soft tissue as fully bounded between each other.

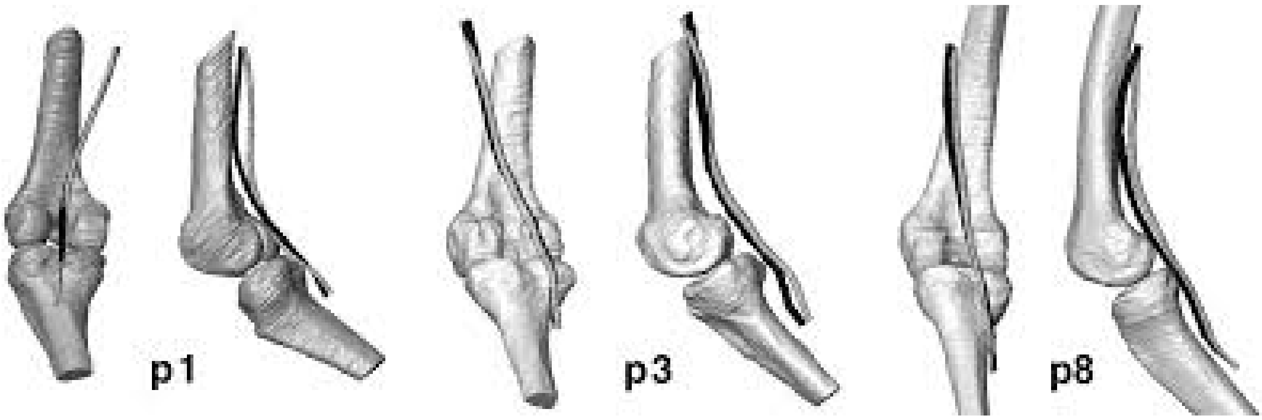

Figure 2.7: Posterior and lateral views of the bent situation. The displacements of the arteries predicted by the numerical model are shown in gray and the displacements acquired on MRA images in black for the patients with a poor (p1) and good (p3) prediction outcome.

Ghriallais 2013

Another improvement on this particular topic come from Ghriallais and Bruzzi (2013) they set an anatomically accurate 3D finite elements model capable of capturing the deformation characteristcs of femoropopliteal artery during knee flexion. They perform images processing and set a finite element analysis. The model consisted of one artery part, 3 bones parts (tibia,femur and patella), 8 muscles parts (adductors, vastus, rectus femoris, gracillis, Sartorius, semimebranosus, semitendinosus and biceps femoris) and an encasing soft tissue part, model showed in Figure 2.8. As results they study shortening, curvature, torsion on the entire leg and they measure also the radial compression, finding close correlation with previous studies existing in literature. Although the big computational cost this model wanted to underline the precision of finite element analysis, more easy to perform compared to other studies. Here we want to underline one of their conclusions, that will have a a key role in our model, and it's that they thought it was impossible to evaluate and apply to the stent the dynamic external forces acting in that region.

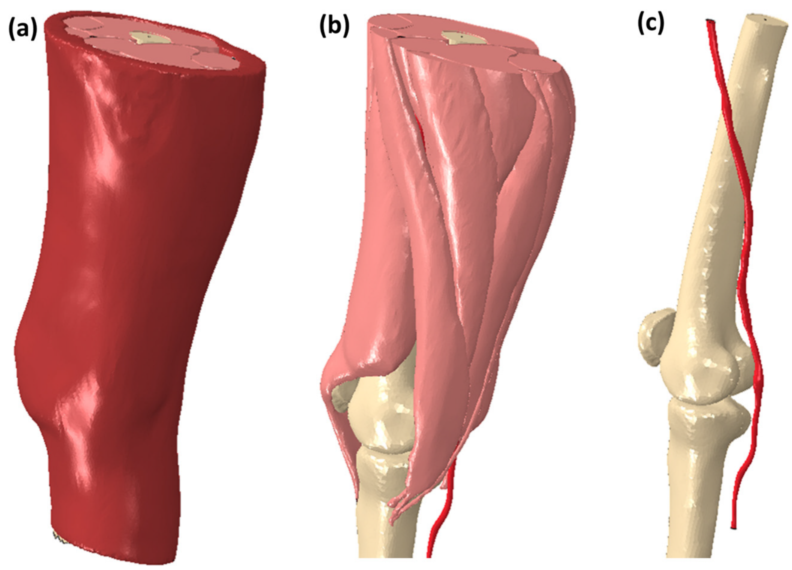

Figure 2.8: Finite element model of the leg: (a) the complete model, (b) outer soft tissue (skin) removed to reveal individual muscles, and (c) outer skin and muscles removed to reveal the underlying bones and femoropopliteal artery.

Ghriallais 2014

One step forward in the last model was made from Ghriallais and Bruzzi (2014) again where they try to simulate a stent deformation adding a stent in their older model, assigning stiffened material to a portion of the artery to represent CORDIS SMART^{TM} nitinol stent. They focus on two different issues: the effect of stent's length, modeling three different length 40 mm 60 mm 90 mm, and effect of stent's position placing a 60 mm stent in distal, middle and proximal SFA, as in Figure 2.9. Again they evaluate, comparing results on different stent, different positions and between stented and unstented artery, shortening, finding that with shorter stent the shortening is greater and also that the shortening increases from proximal to distal; axial twist, the angle decreases with the increasing of stent's length and is greater with stent distal position and lower with stent in proximal position; and curvature which is higher in shorter stent and in proximal SFA. Moreover they find that unstented artery shorten more than stented and also stent reduces axial twist. The main limit here is that simulating stent as arterial stiffening don't take into account the possible slip between arterial on stent.

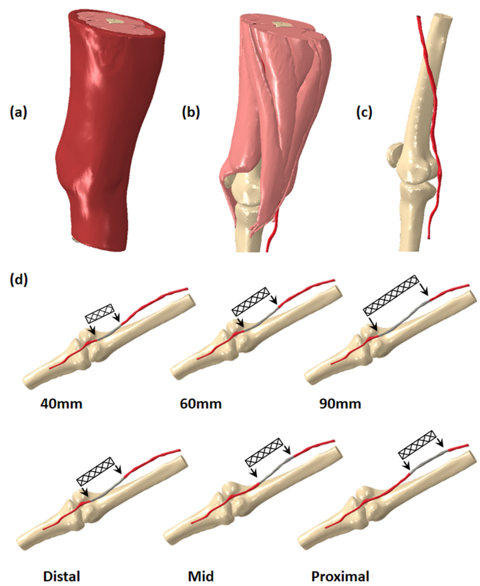

Figure 2.9: Finite element model of the leg and stented femoropopliteal artery: (a) the complete model, (b) outer soft tissue (skin) removed to reveal individual muscles, (c) outer skin and muscles removed to reveal the underlying bones and femoropopliteal artery and (d) geometries of the six stented vessel models including three stent lengths (40 mm, 60 mm, and 90 mm) and three stent locations (distal SFA, mid SFA and proximal SFA).

Petrini 2014

Another interesting study about FEA simulation of peripheral stent is made by a group of Politecnico di Milano, Petrini et al. (2015), where they set a patient specific numerical model, finite elements analysis and fatigue simulation of a stent. They collect patient specific data, literature data and stent characterization and created 3D model of stent and 3D model of vessel (as a cylinder), Figure 2.10. They simulate the stent deployment and fatigue analysis. The proposed numerical approach provides information on fatigue behavior of peripheral NiTi stents and, despite all of the limitations mentioned due principally to the lack of data, this model is able to predict some important results in the patient follow up.

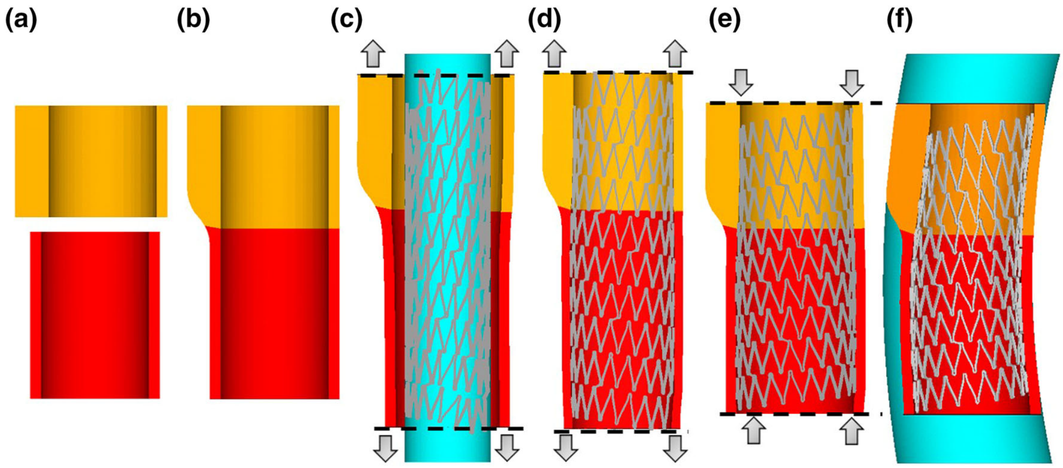

Figure 2.10: Stent deployment and fatigue simulation: (a) two separated tube models of healthy and stenotic artery, here not adopted; (b) 3D FE model of the unloaded vessel representing the steep transition zone; (c) axial pre-stretch of the vessel and stent crimping; (d) stent self-expansion; (e) axial shortening and (f) bending of the vessel.

Conti 2016

In the last years our Group from Pavia University, Conti et al. (2016), implements a structural finite element analysis of popliteal stent based on the kinematic of the artery itself. We analyze a case of a 66 years old man with an aneurysm of the right popliteal artery. After the images processing of CT scan in straight and 40° knee flexion position, and calculated the centerline of both configuration, we impose the displacement field of lumen centerline on a stent model based on a real device, PRECISE® Stent from Cordis. The results are divided in two parts: deformation of the vessel during knee flexion evaluating shortening, curvature and tortuosity, and deformation of the stent. We find some non uniform deformations and stresses, especially in the proximal part of the device, that may induce fractures for the high solicitation or for the overlapping of the stent's struts and the consequent possible fretting corrosion, in Figure 2.11 results are showed. The main assumption that the stent doesn't influence the arterial kinematics but only vice versa may affects the results, but here we want to highlight the importance of structural FEA on stent as a possible pre operative tool of prediction.

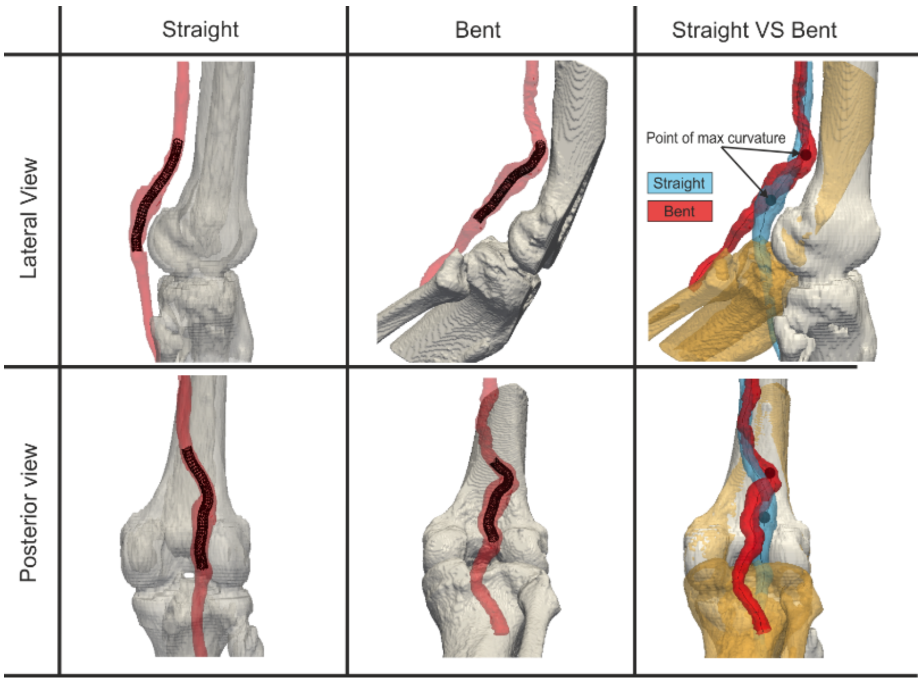

Figure 2.11: Stenting simulation and vessel centerline analysis: different views of the simulated results of stenting for the leg in straight position (left image column), after knee bending (middle image column) and position of the point of maximum curvature in both cases (right column). It is worth noting that the deforming surface imposing the kinematic change is not illustrated here, this motivates the gap between the lumen profile and the stent which is deployed to a reference diameter of 6.8 mm.

2.4 Others

Young 2012

The goal of Young et al. (2012) is to model the key physical characteristics of the vessel, focusing on the arterial length changing during activity. The innovation in this work is the technique of imaging used to get the information: is stead of MRI, CT or arteriography, they use a motion capturing system, a kind of gait analysis system. As a great assumption they decide not to consider mechanical properties of the vessel. The main result is an equation to get the percentage of shortening with a known angle of flexion of the knee.

$$\%F_{shortening} = (0.0016) * \theta HF_{max} - 0.0289 \tag{2.1}$$

Another result that they find is very interesting and need a deeper investigation because it is in contrast with the results of another work. They get as a results, in the opposite way as Wensing et al. (1995) demonstrated, that age factor doesn't influence shortening or elongation.

2.5 Fluid dynamics

This part is not strictly related to our model, but, since I made some researches about fluid dynamics computational model when I was at the UNMC in Omaha for Dr. Kamenskiy, we decided to add here briefly what I found.

Giordana 2005

We have an example of blood flow in bypass related study in the work of Giordana et al. (2005) where they consider the effect of geometrical configuration of a distal anastomoses of a bypass graft on steady flow field, taking geometries from three patients MRI with different angles between the graft and the proximal host vessel, showed in Figure 2.12. Using this non-invasive post-operative procedure for the surveillance of distal anastomosis of in vivo by-pass graft they show how local and global geometric characteristics, curvature and planarity of vessels, have influence on wall shear stress an steady transport of fluid particles.

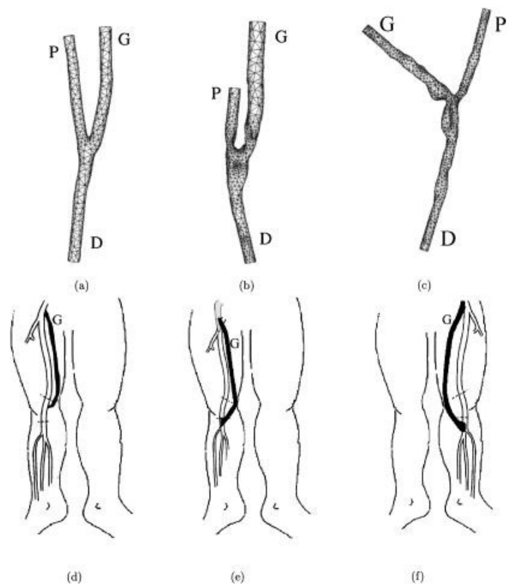

Figure 2.12: High-order computational meshes of the distal anastomosis for (a) study 1, (b) study 2, and (c) study 3. The letters G, P and D denote the graft, the proximal and the distal part of the host vessel respectively. In all the computations presented, the graft is considered as an inflow and the proximal and distal host vessels are outflow vessels. Plots (d), (e) and (f) indicate the graft path for the anastomoses shown in plots (a), (b) and (c) respectively.

Wood 2006

The purpose of the study of Wood et al. (2006) is to measure curvature and tortuosity of superficial femoral artery, with model processed from MRI images of male and female between and below the adductor canal, and their relationship with sex, region and bloodflow, performing a CFD analysis on patient specific geometries. Curvature and tortuosity, strong correlated with disturbed hemodynamics and consequently in pathologies, is much higher in men than in women, related to weight, body mass index or increased body surface area.

Kim 2008

Kim et al. (2008) aim is to evaluate the interaction between vessel compliance and hemodynamics in a patient specific femoral artery bifurcation, as in Figure 2.13, developing a new fluid structure model. This compliant femoral artery model is compared to a rigid model. They evaluate wall shear stress (WSS), oscillatory shear index (OSI), wall shear stress temporal gradient (WSSTG) concluding that compliance does not influence significantly the parameters previously studied in a rigid lumen, but one improvement of the study should be to study longer segment of artery to evaluate effects of compliance in tortuosity.

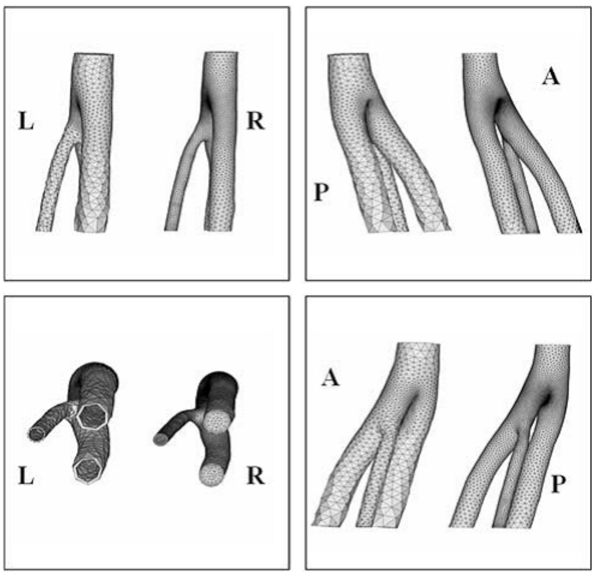

Figure 2.13: Structural (coarse) and fluid (fine) mesh of the femoral artery bifurcation (A: Anterior, P: Posterior, L: Left, R: Right views).

Others

In literature there are many other studies regarding femoropopliteal hemodynamics, such as Liu et al. (2001) and Moayeri and Zendehbudi (2003) that perform computational fluid dynamics taking data from animals' artery, or Rivera et al. (2014) and O'Brien et al. (2015) who study femoropopoliteal's bypass graft hemodynamics using general geometries instead of patient specific model, or McGah et al. (2011) who show the fluid dynamics within a femoral bypass graft using a model taken from real device and a physiologically realistic flow rate.

2.6 Conclusions

All of these studies have brought about improvements in the complex evaluation of femoropopliteal kinematics, biomechanics and stenting, and each one of them has been useful to give us solutions and ideas for our project. In fact the works of Wensing et al. (1995) , Cheng et al. (2006) , Cheng et al. (2010) , Choi et al. (2009) helped us to find the smartest way to get values of deformations of the vessel and gave us a comparison for validating our model. With the very useful collaboration of Dr. Kamenskiy and the University of Nebraska Medical Center (UNMC) group, we had the possibility to work and get data from cadavers and to actually see what is the environment of this region, understand better the real anatomy of the part and consequently have more chance to perfect our work.

In particular from the work of Wensing et al. (1995) and suggestion given from Dr. Kamenskiy about arterial prestretch (Kamenskiy et al., 2016), we based our idea to evaluate the length surplus of the artery and the curvature related to the longitudinal prestretch and consequently the relation with age.

Another interesting idea came out from the work of Ghriallais and Bruzzi (2014) to model a stent stiffen a region of the vessel, so at the end we studied also the relation between the stiffness of the stent region with curvature and length excess of the vessel. The overview of the computational model, discussed above, including our contribution, highlights that the biomechanical analysis of femoropopliteal artery is still an open issue calling for novel solutions with a lower computational cost.

These are the principals aims of the project we will present in the next chapters.

Chapter 3

2D idealised model

3.1 Aim

In this chapter we describe the model that represents the basis of the whole project.
As we can deduce from the previous chapter, many researchers are focusing on femoropopliteal biomechanics and as we mentioned before the main issues in the past studies have been the interaction between stent and artery, the identification of external forces acting in this specific region and the computational cost of the analyisis, often too high.
Here, with this work, we try to overcome the limitations already presented and existing in literature, developing a very simple model based on real patient preoperative CT scans able to predict arterial-stent behavior.
The basic idea is to find a fast and precise way to simulate the deformation of this complex vessel, having patient pre-operative data of straight and bent leg, in order to put a stent in the model and understand how the device can deform and most of all how the behavior of the vessel changes with a stiffer and complex structure in it. The general and final purpose of all of these works and studies is to find a best stent design and best material that can last years without ruptures or failures.

3.2 Materials and methods

In Figure 3.1 we can find the basic concept of the model, as we explained, the principal purpose was to have a rapid and easy tool of prediction, so, finding the best and physically correct approximations was the first and most important step of the whole work.
Writing the Abaqus Input file with a Matlab script (MathWorks, Natick, Mass) we use Abaqus/STD 6.14 (Simulia, Dassault Systèmes, Providence, RI, USA) for the finite element analysis of a model composed by 5 parts: one for the tibia, one for the femur, one for the femoropopliteal artery and two for the thigh and the calf.

Below we will explain the details of the Matlab script and the Abaqus model, then we will talk about the results we find.

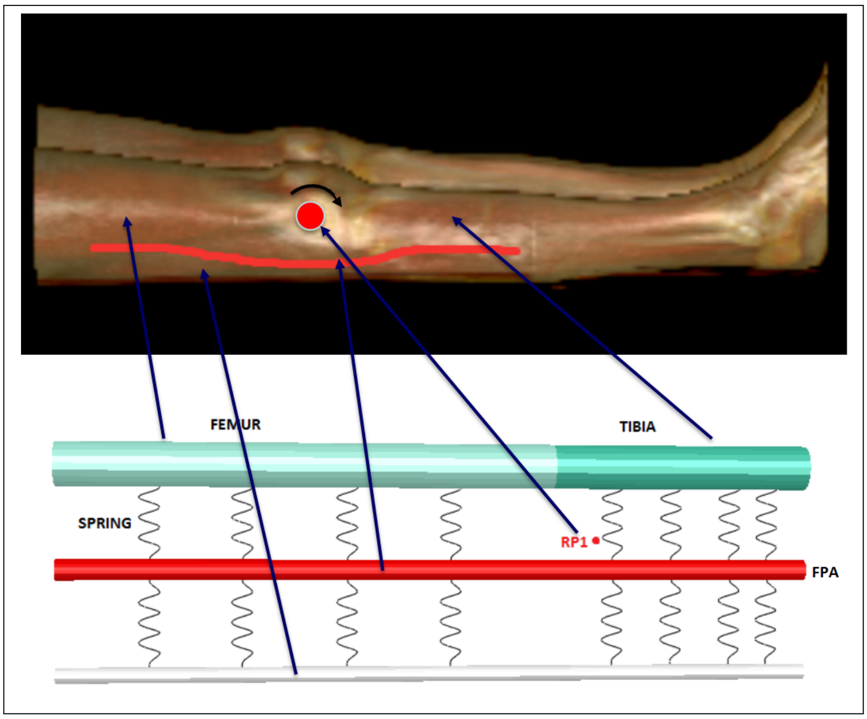

Figure 3.1: Basic concept of the model: we can see the relationship between the anatomic parts and the model parts.

3.2.1 Matlab scripts

So far, we evaluate the influence of increasing of age on arterial behavior during knee bending, following the Kamenskiy et al. (2016) study on arterial prestretch. They measure the difference between the length of the arterial inside the body (in-situ) and the arterial excised, evaluating the dependence with some variables and risk factors. They figure out that the main correlation is with age. They extract the equation we use in our model.

$$\%LPS = -0.00708 * Age + 1.57994 \tag{3.1}$$

After that we study the influence of an increasing of vessel stiffness in a portion of the FPA, modeling a stent in the artery.

The matlab algorithm followed is explained in Figure 3.2. Here the parameters we give are: the coordinates of the Reference Point, which function will be explained in the next section, the length of each part, the length of the different regions that divide the vessel and the bone consequently; in fact we decided to partition the vessel in 3 anatomical region the proximal Superficial Femoral Artery (pSFA), Popliteal Artery (PA) and the distal Superficial Femoral Artery (dSFA). The

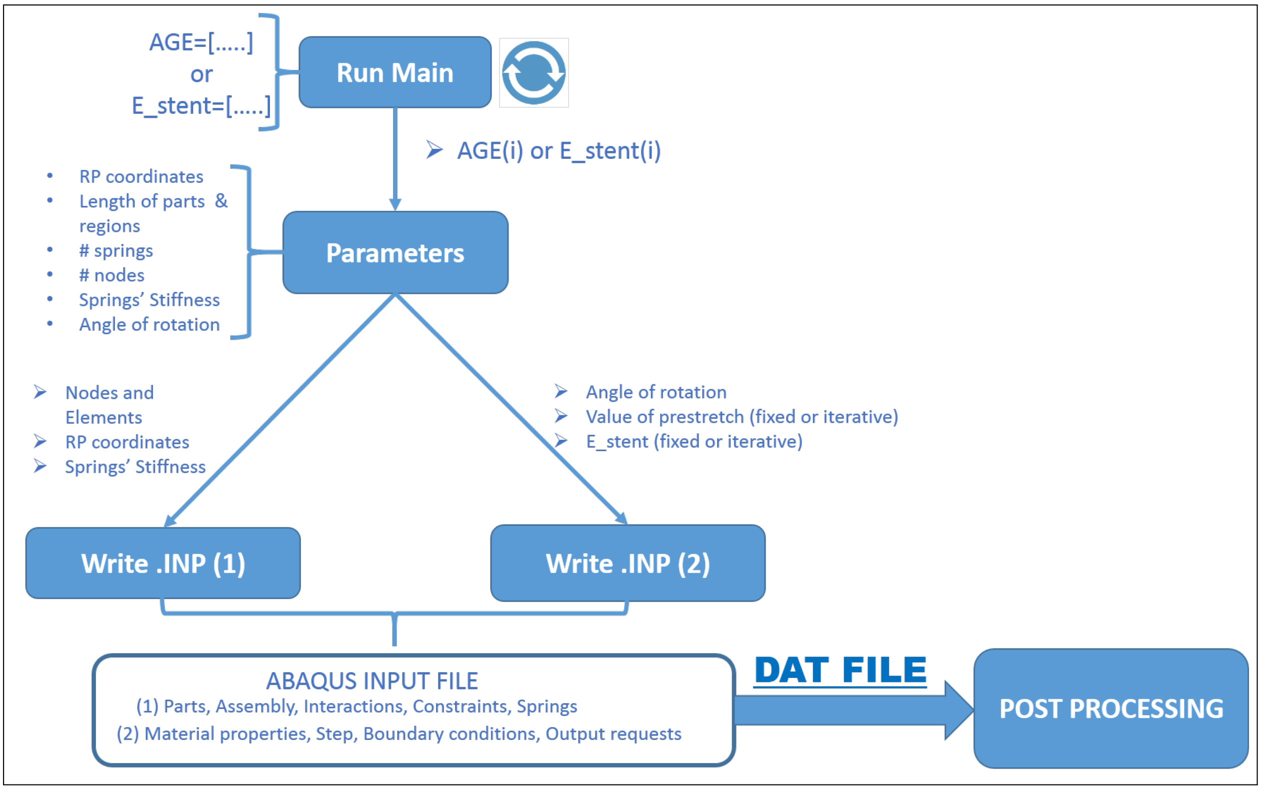

Figure 3.2: The matlab script algorithm.

dimensions of these regions can be evaluated from the CT scan of patient as in Figure 3.3.

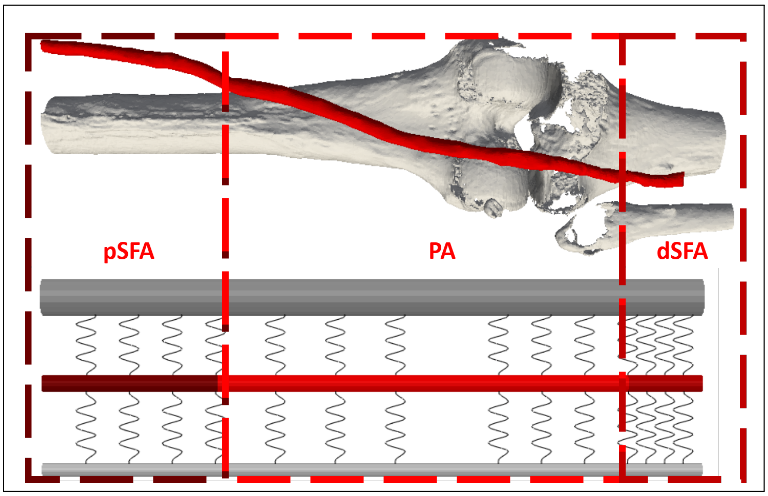

Figure 3.3: Definition of vessel regions: the proximal Superficial Femoral Artery (pSFA) goes until it crosses the bone where becomes Popliteal Artery (PA) and then, right after the knee, it is called again distal Superficial Femoral Artery (dSFA).

Then we give the desired number of springs per region, the number of the mesh nodes between the springs, the stiffness of the springs, dividing them between SFA and PA, thinking about the higher freedom of movement the Popliteal artery has in the popliteal fossa right behind the knee, and finally we give the angle of rotation of the knee.

Defined all the parameters we need, we create the nodes and elements where put the springs on and the nodes and the element of the whole mesh for each part.

After all of this steps we need to actually write the *ABAQUS INPUT FILE*, structure details explained in Appendix A, and for doing this we wrote two matlab functions, then called in the parameters' script. The first of these two takes as input the nodes and the elements defined in the previous script, the values of the springs' stiffness, the coordinates of the reference point and write on a text file the parts with relatives nodes, elements, sets and sections, the assembly of the parts, interactions and constraints between the parts and put the springs on those specific nodes we mentioned before. The other one takes as input the angle of rotation of the knee, the difference between the in-situ length of the vessel and the excised one to perform the arterial prestretch, and the Young Modulus of the region where we might want to model the stent and write on the same text file material properties, steps with boundary condition and some particular output requests such as the one which produces a data file with the coordinates of the nodes of a requested part, in our case the vessel, for each time increment of the simulation, as we are going to see later this will be much useful in the data post processing.

In the next section we will describe extensively the model built in Abaqus and we will explain how the simulation works.

3.2.2 Abaqus model

We decided, for the sake of clarity, to organize this section in the same order as is in the software's interface, so we will describe the parts of the model, the material properties, the type of steps used, the interaction between the part, the boundary condition imposed and finally the first result of FE analysis. We choose 5 *BEAM* element (type *B21*), *BEAM* elements follow the beam theory and they are the one-dimensional approximation of three-dimensional continuum all with a *CIRCULAR* section, (DassaultSystèmes, 2014) one is for the Femur, one for the Tibia, one for the Femoropopliteal artery (FPA) and the two others , under the vessel, modeling the encasing of the leg, to resemble the lower boundary of the thigh and the calf.
One of the first doubt was about the cross section of the vessel, it is obvious that a vessel is more similar to a pipe section than a circular one but, thinking of the pressure of the bloodflow inside an in vivo vessel we decide to use a full section. All the cross sections have a constant diameter, 17 mm for the bone, 8 mm for the FPA and 6 mm for the encasing. The average diameter of bone and vessel and length of each one for this first model have been evaluated from the segmentation and 3D modeling of CT scans of a cadaver received from Dr. Kamenskiy group of research (UNMC), and they can obviously change along with each patient. Moreover the lengths are, initially, shorter than the ones measured on the real anatomy in order to simulate the arterial prestretch, in particular in addition to the vessel we shorten also the femur; otherwise the springs attached to the parts, the function of which will be explained in a while, would impose an unwanted reaction force at the beginning of the simulation.
Again, for sake of simplicity and for reduce more the computational cost, althought we know that, expecially for the vessel, the use of an anisotropic hyperelastic material is more appropriate, here we decide to assume, for all of the parts, a linear elastic behavior. In particular bones and encasing have a Young modulus (E) of 18 Gpa and a Poisson ratio (ν) of 0.2, values took from Ghriallais and Bruzzi (2013) and the FPA has an E=2 Mpa and ν =0.33, from Schmidt et al. (2006). Moreover, to get some interesting results about stent deformation in the artery, we create a third linear elastic material to assign on a defined section of the vessel with a variable young modulus that, in an iterative process, get stiffer and stiffer. This let us evaluate the possible arterial behavior change when the stent is deployed in it.
It is worth notice that we are not so much interested in bone and encasing material behavior but only in the vessel one, so we use a particular value for the Young modulus in those parts but actually it has only to be mucher higher than the FPA's modulus, ideally infinite.
The next idea that came out was to modeling, in the assembly section, the external reaction forces acting in the region with springs, in particular we use Abaqus *SpringA element.* Spring element can couple a force with a relative displacement and in particular the element *springA* acts between

two nodes, with its line of action being the line joining the two nodes, so this line of action can rotate in large-displacement analysis, for more information see the Abaqus 6.14 documentation (DassaultSystèmes, 2014).

We connect with springs specific nodes of the vessel superiorly with femur and tibia and inferiorly with thight and calf, as we explained in the previous section, regions corresponding to the pSFA and dSFA have a higher springs' stiffness than the ones in the region of the popliteal artery, where anatomically the artery is more free to move.

In order to simulate the rotation of the knee we use a *Reference Point*(RP), attached to the tibia and to the calf with a *Multi Point Constraint* (MPC), that allow to constraint different degree of freedom of the model; here we choose the *MPC BEAM* that constraints the displacement and rotation of the first node to the displacement and rotation of the second node, corresponding to the presence of a rigid beam between the two nodes, (DassaultSystèmes, 2014). Giving the desired rotation angle to the RP this make the two connected beam rotate, this point will be clarified in Figure 3.4.

Hence we have to define the type of the analysis. The simulation is structured in two steps both

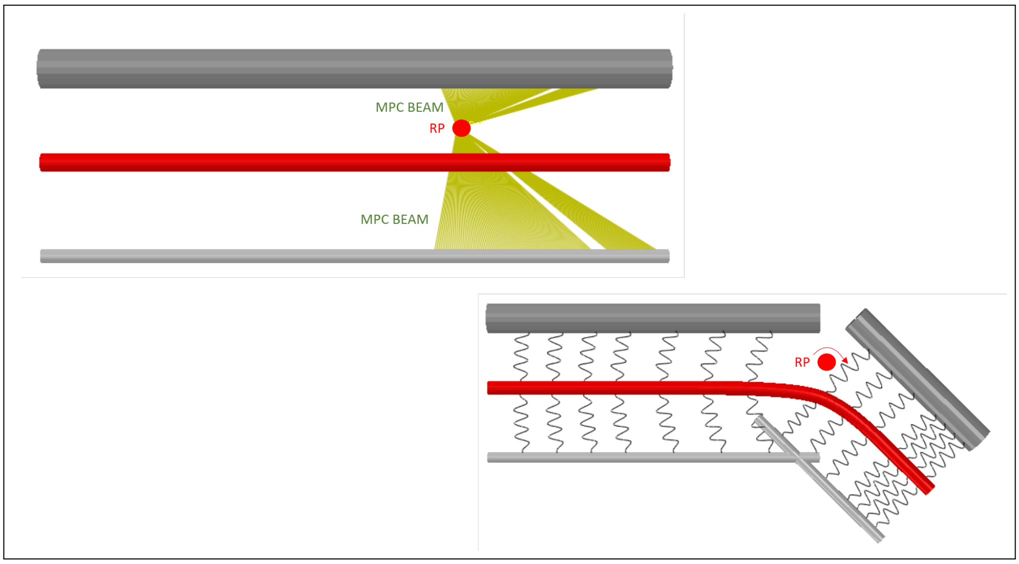

Figure 3.4: The reference point is attached to the tibia and the calf with an *MPC BEAM*, imposing a rotation to this point the tibia and the calf will rotate, modeling the knee flexion. In the figure is showed an example of a 45° degree rotation about the horizontal axis.

Static General with large deformations involved; the first is the prestretch's step, where we stretch the artery until the in-situ dimension, the second is the bending step, where we impose a defined rotation to the reference point and so the tibia will rotate of the same angle to the femur. About interaction, besides the *MPC BEAM* connecting the *reference point* to the tibia and the calf, we impose another *MPC BEAM* between the last node of the tibia and the last node of the FPA, in this way the vessel last node will always reach the same desired position after the knee bending.

To get some significantly results we need to choose the better combination of boundary conditions for each of the two steps. In the first one we use an encastre constraint for the first nodes of femur, vessel and thigh, and then we impose a stretch along X axis, depending on the value of the prestretch calculated, to the femur, the thigh, the reference point and obviously to the vessel. In the second we mostly leave the same condition of the step before, changing only the boundary conditions on the last node of the vessel, removing them all, and obviously imposing the rotation value to the reference point, which is the purpose of this step. The mesh is, as already said, a *B21*, i.e., A 2-node linear beam in a plane.
At the end we set up a *full analysis* and finally we run the simulation, the result is depicted in Figure 3.5. For each simulation we got a Dat file containing the coordinates of FPA part per each time step of the simulation and in the next section we will explained how this coordinates will be used.

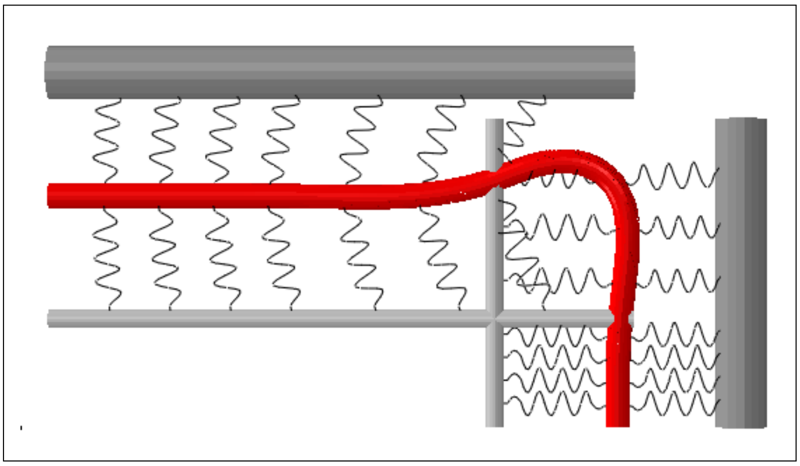

Figure 3.5: General result of the simulation with a 90° angle of rotation.

3.2.3 Post processing

The last part of the process is the data elaboration and post processing. For doing this we wrote a matlab script that reads each one of the data file coming from the iterative simulations and extracts the coordinates of the deformed vessel in the last time step, i.e., the final result of the analysis.
These simulations, until now, may vary for different age (therefore different prestretch values) or different Young modulus in the region assigned to the stent, going from the absence of stent, same stiffness of the rest of the vessel, to a much higher elastic modulus.
Once we get the analysis data, we build the shorter path, that is the distance the vessel would cover if it were a straight tube instead of a tortuous one (Wensing et al., 1995) as defined in Figure 3.6, going from the first and the last node of the deformed vessel, those points, due to

constraints and boundary conditions, remain always the same in every case so the shorter path does not change. With this value we calculate the difference between the vessel part length and the shorter path length as a first measure of tortuosity.

Then we use a function to calculate the curvature of the vessel and see how it changes between the

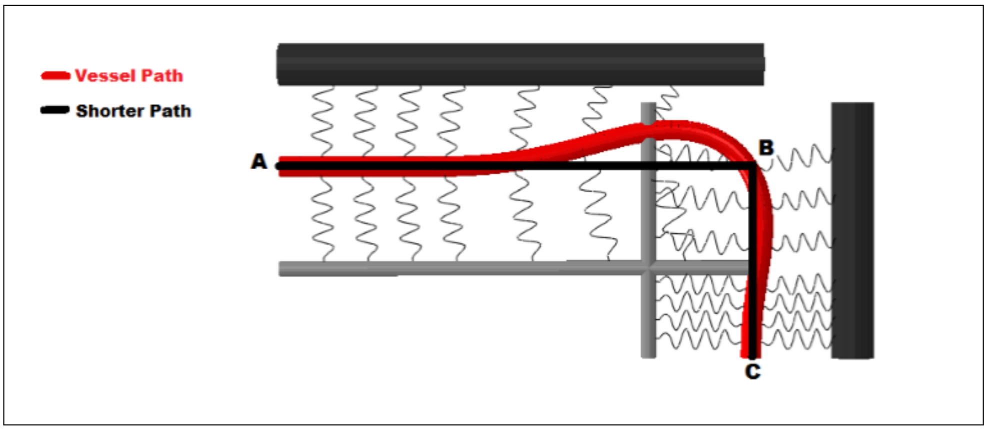

Figure 3.6: Shorter path vs vessel path.

different cases. This function actually fits a polygons to the points and then calculates curvature following the parametric equation below. We adapt the equation extracted from (Pressley, 2010) for a 2 dimensional case.

$$k = \frac{\dot{x}\ddot{y} - \dot{y}\ddot{x}}{(\dot{x}^2\dot{y}^2)^{\frac{3}{2}}} \tag{3.2}$$

At the end we produce some plots we will discuss about in the results section.

3.3 Results and discussion

In the following, we present the results of our 2D model focusing our attention principally on two issues: the change in arterial deformation due to different ages and the change due to different elastic modulus in the region assigned to the stent, and we compare them with some previous work existing in literature.

3.3.1 Effect of age and longitudinal prestretch

In the post processing script we elaborate data producing some interesting plot regarding the effect of age, and the consequent different values of prestretch (Kamenskiy et al., 2016), on the length surplus and curvature of our vessel model.

About the length surplus, we based our study on the work of Wensing et al. (1995) where they perform a series of geometric calculation to evaluate arterial tortuosity. They study the length surplus due to the smooth bending of the artery during knee bending.

In our work we try to perform similar measurements on the model in order to see if it can give some interesting result despite its simplicity.

As we can se in Figure 3.7, we perform seven simulations, from 20 years to 80, with a 90° knee bending and we calculate the length surplus as the difference between the length of each deformed vessel path with the length of the shorter path, as in the equation below

$$LS = \left(\frac{vessel\ path - shorter\ path}{shorter\ path}\right) * 100 \tag{3.3}$$

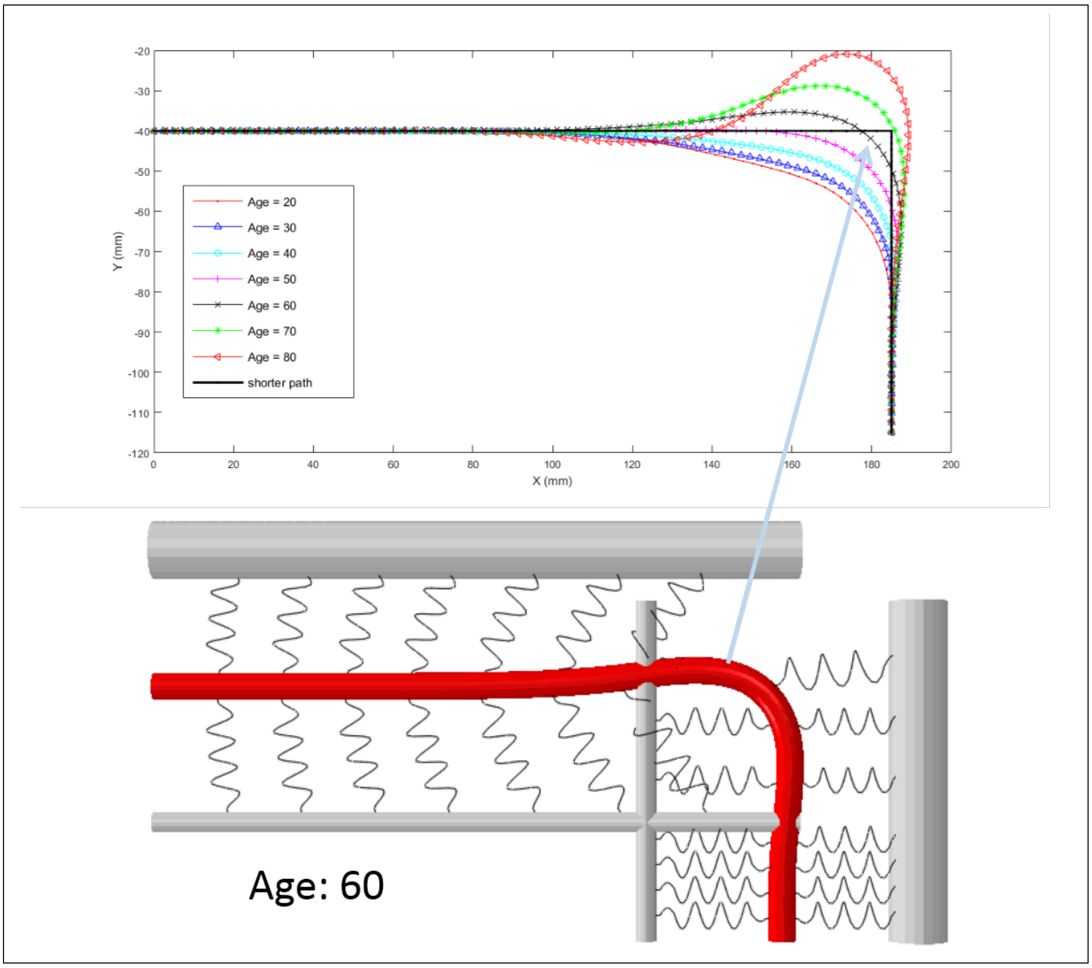

Figure 3.7: In this plot we can see the shorter path and the result of every simulation per age. we take as example a 60 years model with a knee bending of 90°.

from these calculations we got the result depicted in Figure 3.8. As we can easily see the trend

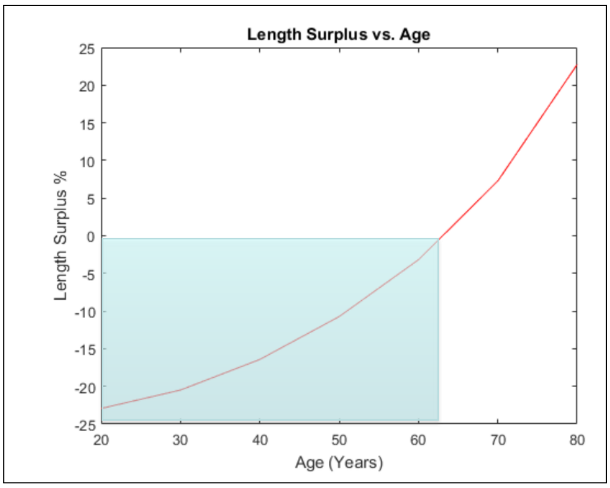

Figure 3.8: Length Surplus VS Age. The length surplus increases with age, this is reasonable because increasing age the longitudinal prestretch decreases so the artery can't accommodate the foreshortening and bends more.

of these data shows that the length surplus increases with age exponentially, so the tortuosity increases, this makes sense if we think about the study of Kamenskiy et al. (2016) about prestretch, in fact as we can see in their plot in Figure 3.9, the longitudinal prestretch decreases with age, so the artery can accommodate less the shortening that occurs during knee bending and consequently it bends more.

This outcome also totally agrees with the study of Wensing et al. (1995), even though apparently

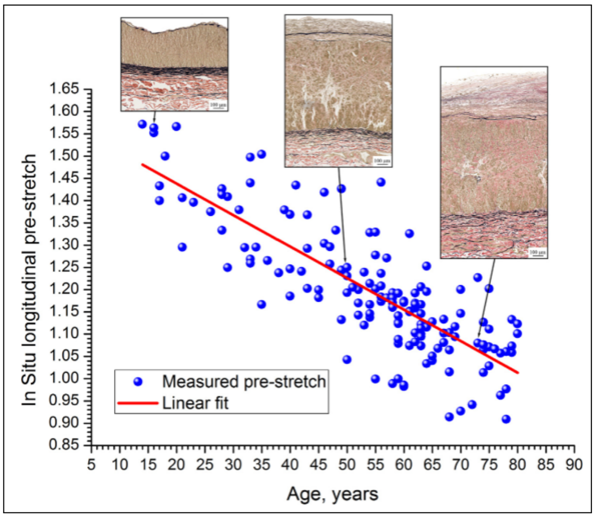

Figure 3.9: Longitudinal PreStretch = - 0.00708 * Age + 1.57994. (Kamenskiy et al., 2016).

they say the length excess diminishes with age but it is because they measure it in a different way, in fact they evaluate that in older people artery makes more efficient use of space available, this

means that artery curves more and more sharply and tortuosity increases dramatically.
We also evaluate the relationship between curvature and age in Figure 3.10, from this plot we understand that also curvature increases with age and moreover we can see that all of the peaks are near the knee in the popliteal region, in fact it's the region where the artery is more free to move and bends more.

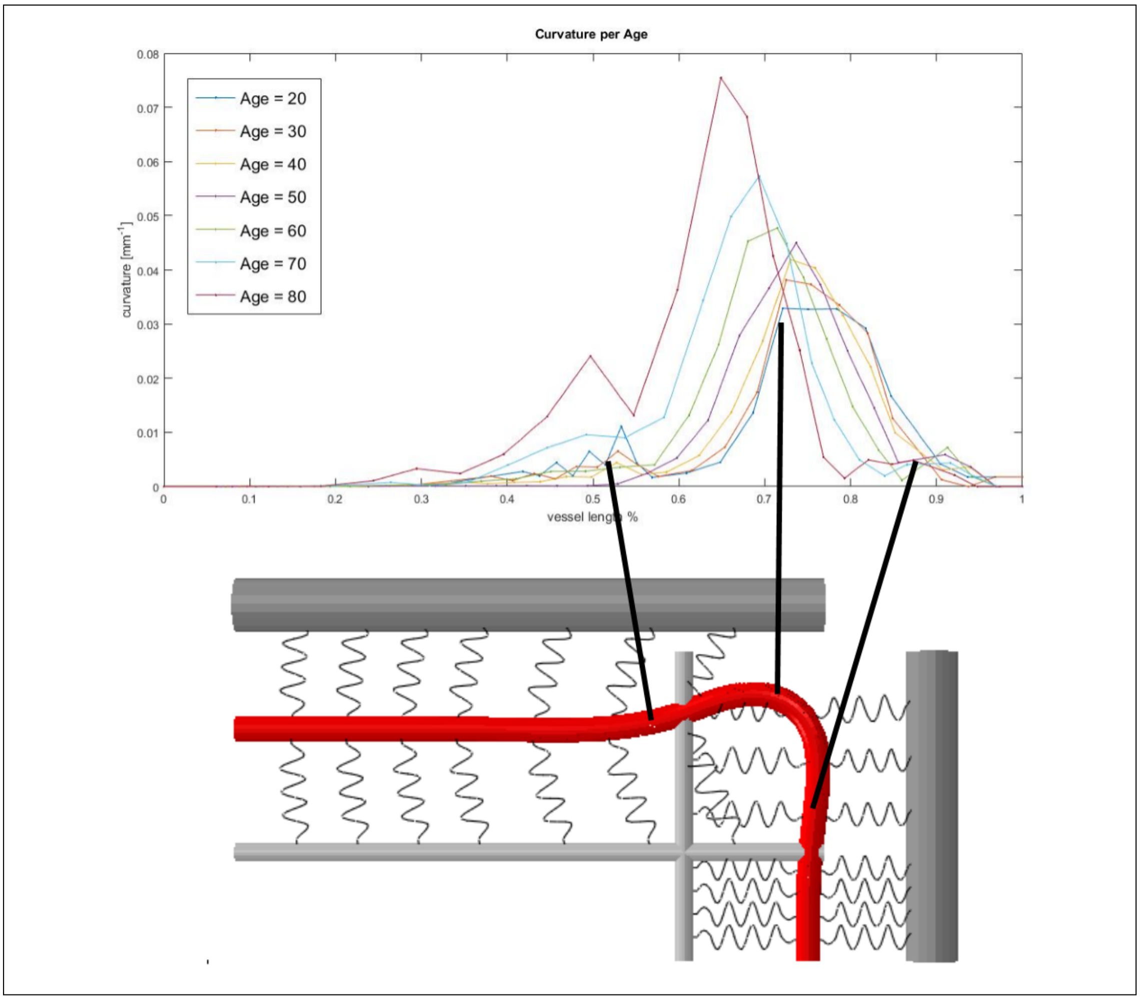

Figure 3.10: Curvature on the deformed vessel. In each curve it is possible to see the higher peak just above the knee, as we expected.

All of these results lead to the conclusion that the deformation of the artery, especially in older people, could be fatal for a stiffer and less able to bend stent device deployed in it, but it's a matter of fact that atherosclerotic pathologies occur more in elderly people, this is why all of this studies have a great relevance in order to improve technologies and this is also the reason why we extract the results coming in the next paragraph.

3.3.2 Effect of a stiffer region in the artery: stent

We implement the stent/vessel interaction simulation increasing stiffness in a region of the artery, in particular the popliteal artery. So we perform again 11 simulations, in Figure 3.11, with a stiffness goes from 2 Mpa (i.e., absence of the stent) to 202 Mpa, a knee bending of 90° and a fixed age of 70 years, comparing them again with the same shorter path.

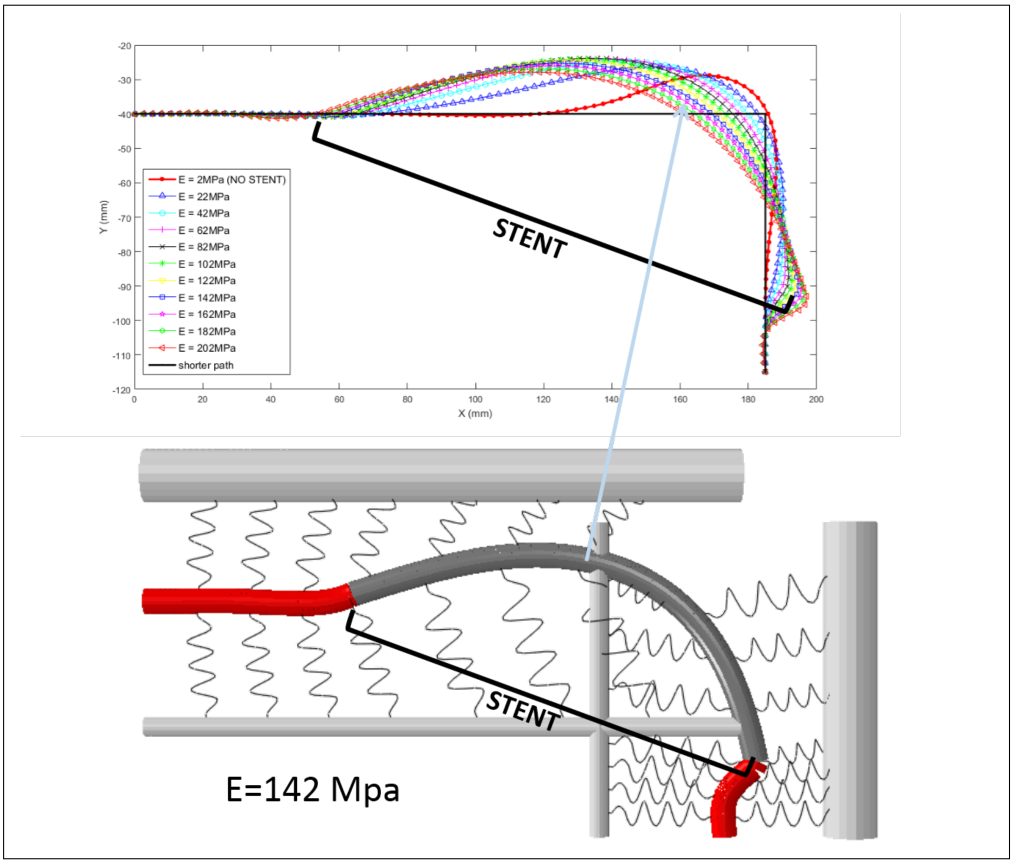

Figure 3.11: In the plot we have the shorter path and the result of every simulation per different stent stiffness. As a model example we choose a stiffness of 142 Mpa.

Here, contrary to before, the length surplus diminishes with age, Figure 3.12. This is correct because with a stiffer region in it, the artery can bend less and accomodate less the shortening. This is also the topic of the studies of Smouse et al. (2005), they highlight that a stiffer region that altering the axial rigidity of the vessel may reduce the arterial ability to accomodate foreshortening, but, since the amount of shortening of the artery during knee flexion will remanin the same, so the artery will bend and undulate more at the adjacent unstented artery, increasing bending of the vessel in those regions and adding stress that may be the cause of stent kinking or fracturing. In

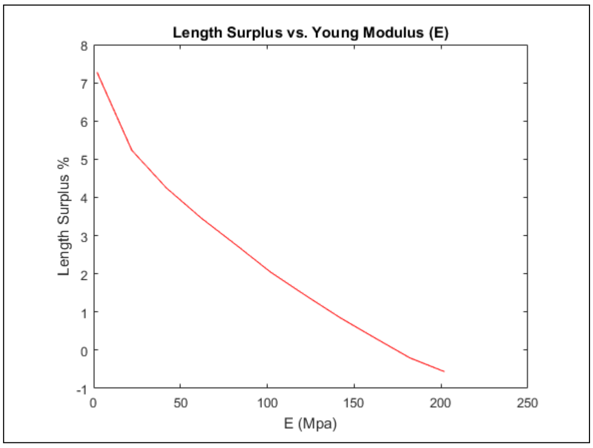

Figure 3.12: Length surplus VS Young modulus of popliteal region. The length surplus decreases with stiffness, because the vessel can bend lesser and lesser with the increasing of stiffness.

our model we find the same outcomes and we can see them also in Figure 3.13, where it is worth notice how the curvature decreases within a stiffer popliteal artery and increases rapidly at the edge of the stent.

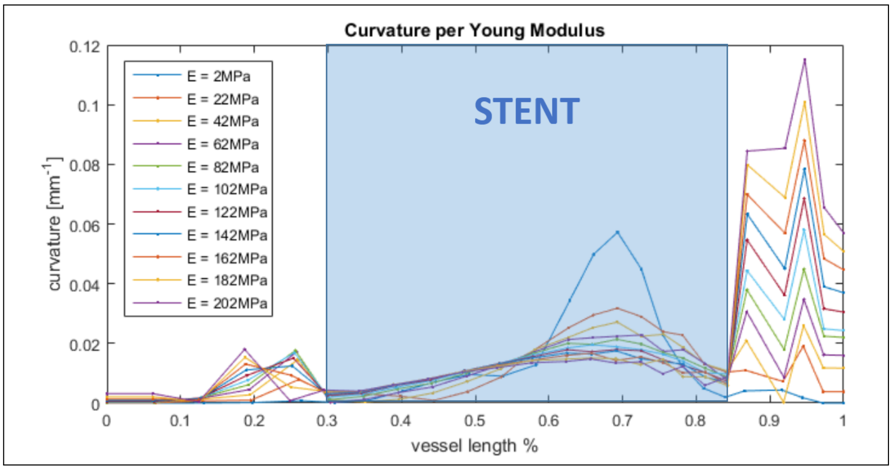

Figure 3.13: Curvature per Young modulus. The curvature's values decrease with E in the stented region and, at the opposite, increase drastically at the extremities of the stent. In blue is highlighted the stiffer region.

3.4 Limitations

The 2D background could define the main limitation of this present model, in fact the vessel during knee flexion physiologically curves even in the third dimension. This lack of information can influence even the behavior of artery depending on age, because, expecially where the artery pass through the abductor hiatus, we probably have nonplanar bending and this bending might become stronger in older people (Wensing et al., 1995), and can influence also the behavior of the stent, in fact as we can see in the work of Smouse et al. (2005), stents placed into the popliteal artery undergo varying degrees of morphological changes with joint bending and can shift, bend and also kink causing ruptures of the devices or damages to the arterial wall.
The second limitation is the lack of specificity of this first model. Properties and behavior of FPA can change a lot within patient (Cheng et al., 2006), the result in curvature are definitely influenced by the differences between patients' straight leg configuration, vessel rigidity, diameter, surrounding tissues and muscles, pathologies and even the patients' lifestyle and habits.
Our modeling does not take into account the slipping effect between the stent and the arterial wall; such an effect cannot be reproduced by our approach, calling for a more complex analysis accounting for contact modeling of the two structures. It is worth mentioning that also previous studies in literature, adopting complex 3D modeling, such the one of Ghriallais and Bruzzi (2014), are neglecting this aspect.
In the next chapters we try to overcome partially of these limitations implementing two different models, the first in 2 dimensions but with an increased patient specificity and in the second we add the third dimension, it is therefore able to catch even the out of plane deformations of the vessel.

3.5 Conclusions

We showed how our model, with a total CPU time of less than ten seconds on a Processor 2,9 GHz Intel Core i7 and a number of nodes lower than 1000, can catch the main features of FPA behavior and can even give some interesting results about stent and artery interaction. We saw how the increasing or decreasing of length surplus follow the theory already validated in literature, how the curvature changes according to previous studies between different age and with the present or absence of a stiffer region inside it, and this is very interesting thinking about how the model is structured and how fast is the analysis.
The further improvements will see the increasing of patient specificity of the model, moving also in a 3D environment. In the next chapters we will present how we implement our patient specific models, with some preliminary results.

Chapter 4

From 2D to 3D patient specific modeling

4.1 Materials and methods

In this chapter we present our 2D patient specific model depicted in Figure 4.1, as we said before here we improve the patient specificity even though we work yet in a 2 dimensional environment. At the end of the chapter we introduce also the 3D patient specific model, with some preliminary results.

Compared to the model before here we take information about centerline and diameters directly from the CT scan of the patient, for this analysis we use images and data of a 66 years old man with a aneurysm of the right popliteal artery, taken from our previous work (Conti et al., 2016) and received from Dr Michele Marconi, vascular unit of Cisanello hospital in Pisa.

Hence, we get the stl models of bone and vessel in the extended leg and knee flexed configurations created in ITK-snap using the method *Snake evolution* (Yushkevich et al., 2006) and registered one onto the other using the module *vmtkicpregistration* of Vascular Model Toolkit library (VMTK - www.vmtk.org). Then we move them in the same reference system of the model, finally we extract from VMTK centerline's coordinates and best fitted vessel's diameters in both configurations.

Below we describe the framework of this new part of the project, following the same organization of the previous chapter.

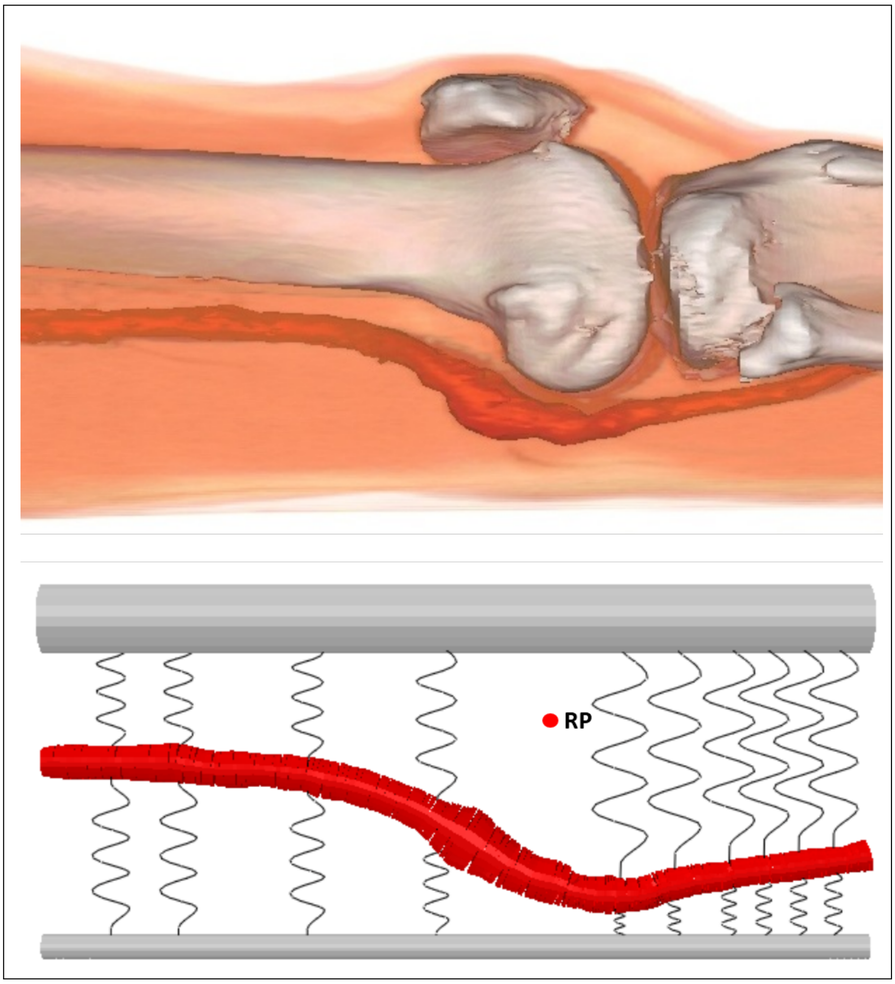

Figure 4.1: 2D patient specific model, at the top of the figure we show the volume rendering of the leg with the 3D model of bone and vessel, at the bottom our model with the patient's centerline and diameters. It is worth noting that in this picture, for sake of clarity, we don't implement prestretch, otherwise the undeformed model should be shorter than the real anatomy. Once the artery part of the model is prestretched does not follow anymore the real patient's centerline, we will discuss this issues in the discussion's section.

4.1.1 Matlab scripts

The structure of the scripts is almost the same of the 2D general model, we have the parameters' code that calls the two functions for writing the Abaqus input file.
In parameters' script the input data given are, as in the other previous script, length of parts, length of regions, number of springs, number of nodes, coordinates of the *reference point*, the angle of rotation, 40° in the Pisa's patient case, age and value of the longitudinal prestretch (Kamenskiy et al., 2016), equal to 1.11 for a 66 years old man. As before we implement the arterial prestretch shortening the vessel, the femur and the thigh parts and moving backward also the *reference point*. One of the two changes here is in loading the coordinates of the two centerlines; on the existing straight vessel part of the general model we change the Y coordinates, all equal to zero at the beginning, with the patient specific ones, obviously relative to the extended leg, creating the new patient specific vessel part. The model is also now able to take into account the variability of arterial radius along its length; this improvement is particular important when modeling of aneurysm or arterial tapering are considered. In this script we also calculate the displacement between the last node of the vessel part of the model at the beginning of the simulation, that means not yet prestretched, and the last node of the patient real flexed leg centerline, this is used to set an additional boundary condition we explain in the next section and is given as an input parameter to the second *Write .INP* function.
In order to read the centerline coordinates file, we use another Matlab script that extracts this data and save them in a Matlab workspace. The Figure 4.2 explain the algorithm we followed.

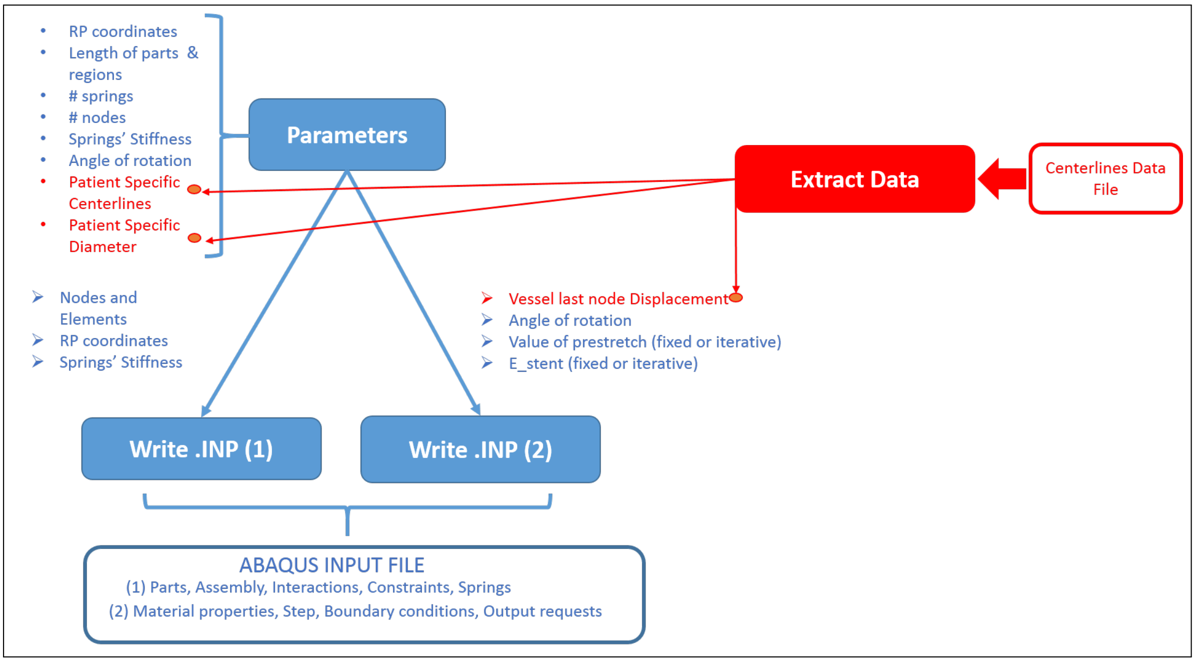

Figure 4.2: The matlab script algorithm for the new 2D patient specific model.

4.1.2 Abaqus

Here, again, we will describe briefly the FE model following the Abaqus interface scheme, focusing expecially on the changes we make compared with the previous one.
We still have the same 5 beam elements, (*B21*), and the *reference point*, assembled in the same way as before, the only thing changed is the vessel's part, because now is not a straight cylinder anymore but follows the patient centerline in the extended leg configuration and has the patient vessel's diameters.
We use also the same linear elastic materials even for bones and for the vessel and, at the moment, we don't implement the stent simulation so we don't need to add the stent material's properties.
We have the same *springA* elements to model tissues and muscles, with the same stiffness values.
The two steps are setted as in previous model, the first for the prestretch and the second for the knee flexion.
In the interaction between the parts, we still put the two *MPC BEAM* between the *reference point* and tibia/calf but we don't have the *MPC BEAM* that connects the last node of the vessel to the last of the tibia, this is because in boundary conditions we want to impose, in the second step, to the last node of the artery, the displacement, mentioned before, measured from patient's vessel centerline and force the node to go in the same position as it is in real anatomy, increasing the specificity. This is the only boundary condition that changes from the previous model in both steps.
Finally we run the simulation and we show the results in the next section.

4.2 Discussion

In Figure 4.3 we present the result of our finite elements analysis, in this 2D patient specific case. As we can see from the image, is really interesting how adding only the centerline, the diameter

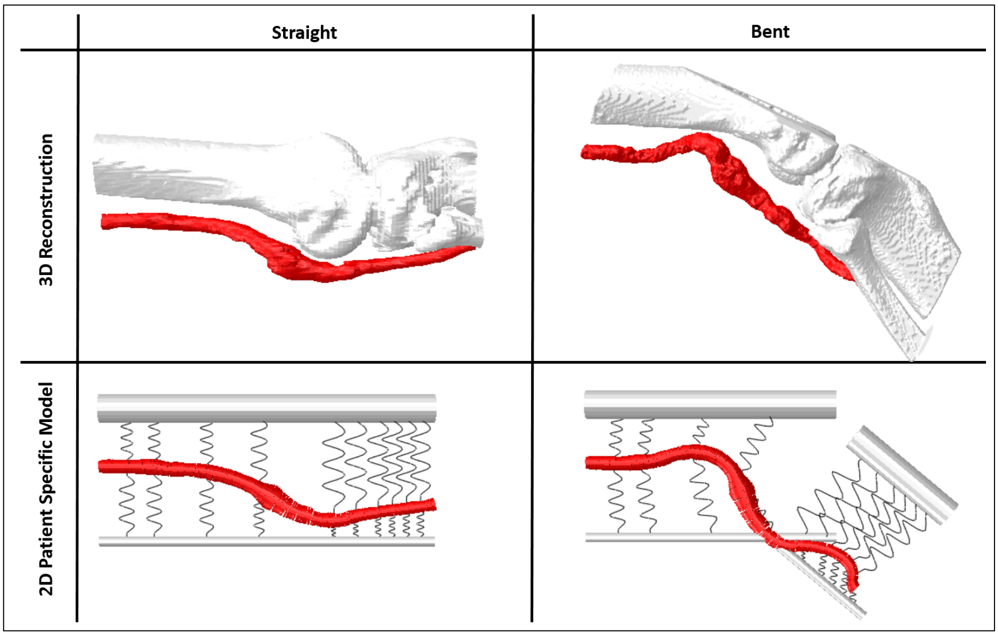

Figure 4.3: Patient CT scans reconstruction (at the top), result of simulation (at the bottom). In the left column we have the straight leg, now the model is depicted at the beginning of the simulation before the prestretch, in the right column we have the leg and the model after 40° knee flexion.

and the boundary condition on the last vessel's node the result of the model is so close to the real configuration. With a very low computational time cost, still less then 10 seconds, on a simple computer, we can get very close to simulate the real physiologic deformation of this complex vessel, in Figure 4.4 we can see our model overlapped to the patient 3D model reconstruction.

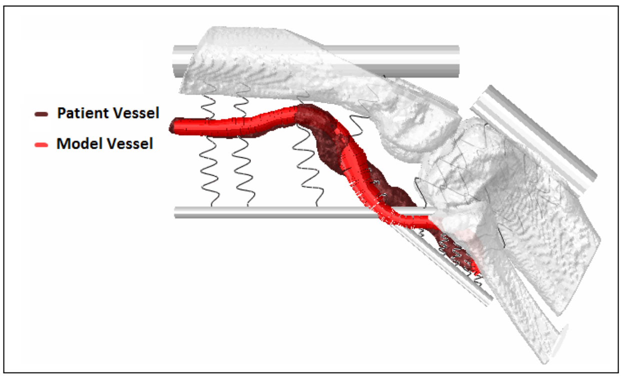

Figure 4.4: 2D patient specific model onto 3D STL model. We can se in bright red the vessel part of the model and darker the anatomic reconstruction of the real artery in the bent leg configuration.

Our result in curvature, Figure 4.5, shows three main bending, the first and the second higher curvature values are right above the knee, as in real anatomy, where the vessel accommodates the shortening due to knee flexion (Conti et al., 2016), the third bending, at the lower extremity of the vessel, seems different from the real anatomy, here comes out the first limitation of this model: the 2 dimensional environment.

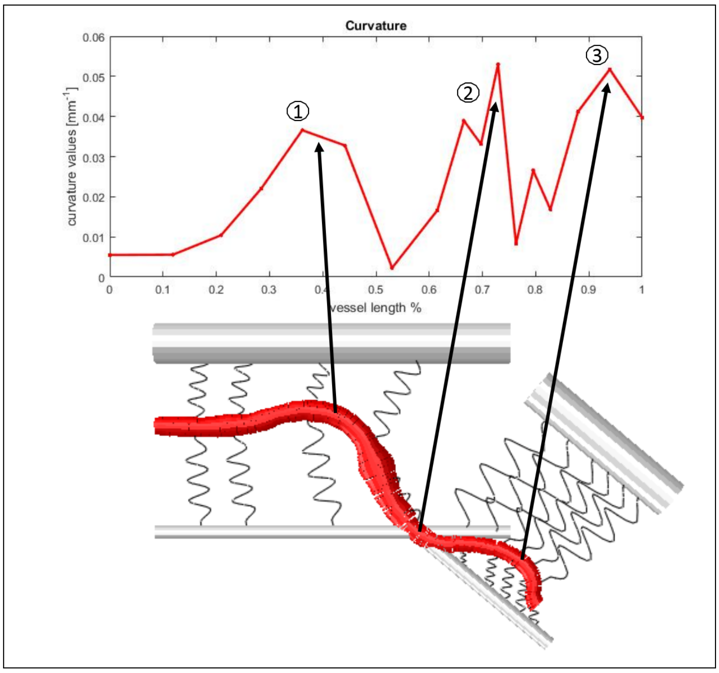

Figure 4.5: Plot of curvature per length of the vessel. we have two peaks, 1 and 2, above the knee and the third at the lower extremity of the vessel.

In real knee flexion, the artery accommodates shortening also with out of plane bending, depicted in Figure 4.6, even severe, that our model so far is not able to catch.
This issue could be crucial in order to reach the best deformed solution and use our model to predict arterial/stent real behavior, this is why we implement the 3D model we present in the next section.
Another interesting thing of our model is that we can modify the angle of rotation of the knee.

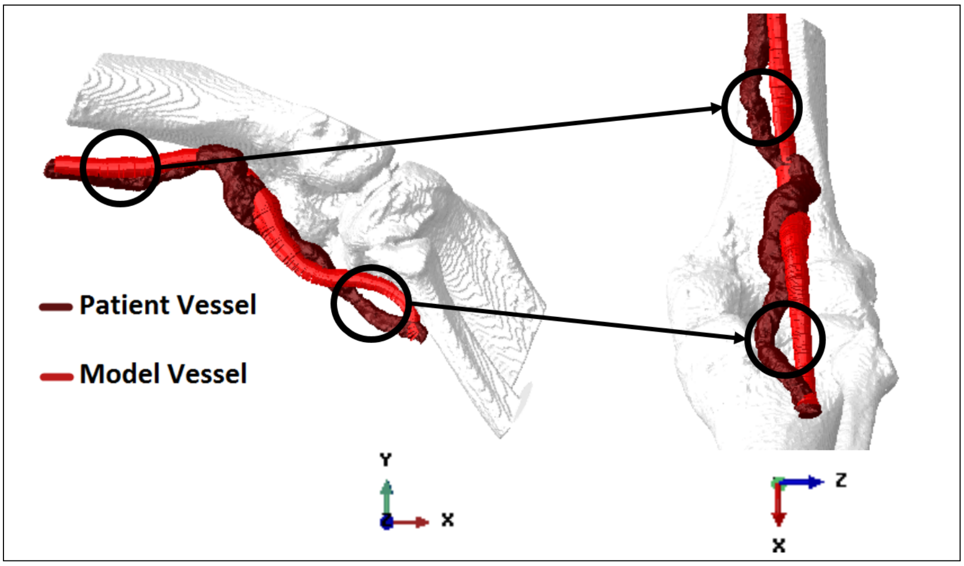

Figure 4.6: On the left we have the lateral view of the two vessels overlapped, on the right the posterior view. We higlight the main out of plane bending of the real anatomy, and so the biggest errors of our model.

This tool, once optimized on patients pre-operative data, with the addition of the stent stiffness model seen in the third chapter, will hopefully allow the user to predict with a certain accuracy how much the stent could change the arterial deformation during knee flexion and how much the stiffer part modeling the device can be stressed without making severe kinking or ruptures, giving some very important, and most of all very immediate, information for a possible treatment with stent in this complex region, that is the final purpose of all the project.
In Figure 4.7 we can observe the results of the analysis for four different angles of rotation, the first is the one presented so far and the only one we have the CT scan, about the others we have to notice that we don't have any patient information for comparing the result and most of all we don't have the coordinates of the real vessel position, hence we can't set the boundary condition on the last node of the vessel part, we use instead an *MPC BEAM* between the last node of the tibia and the last node of the vessel, as we do in the 2D idealized model, loosing a little bit of specificity.
Talking about the arterial prestretch, we have to highlight one issue that is still unsolved, as we can see in Figure 4.8, once the artery is prestretched, at the end of the first step of the analysis,

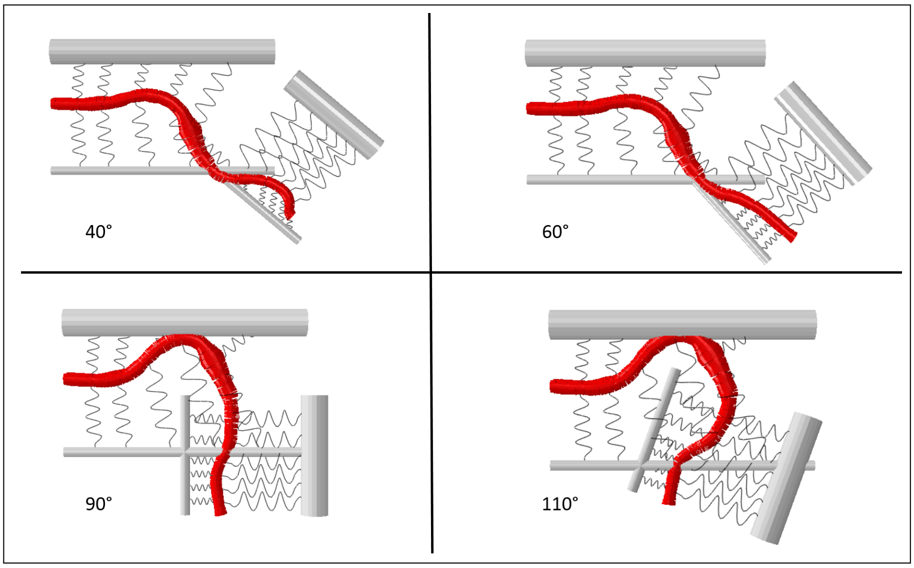

Figure 4.7: view of four different knee flexion, we have 40° rotation, 60°, 90° and 110°

does not follow the real configuration of patient's vessel, this is because, as we implemented the prestretch, pulling the last node until it reaches the real length, the artery part does not elongate uniformly. This error can affect the result because at the moment of bending the artery is a bit different from the patient specific one, and for this reason can curves and bends in others ways. We didn't find yet any clever method for imposing arterial prestretch in a way that could induce an uniform deformation along the artery, but it is one of the many future improvements we want to make in the model. Of all of the listed limitations, as first step, we try to overcome of the 3

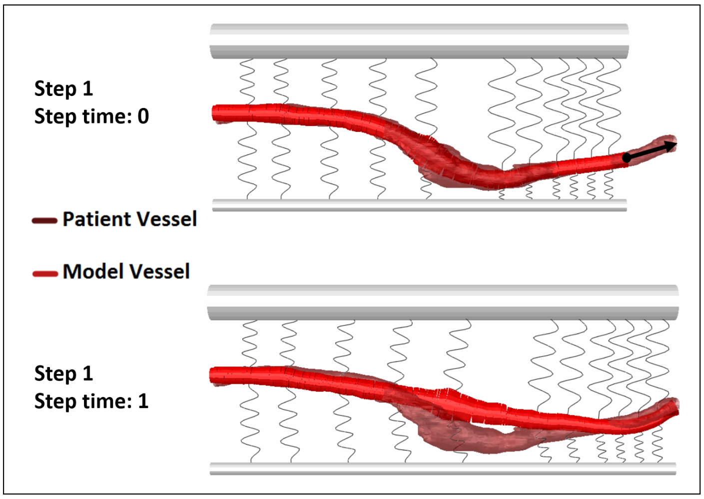

Figure 4.8: First step of the analysis, prestretch's step, at the top we have the undeformed model and at the bottom the prestretched model at the last time step. The prestretched artery is not totally overlapped to the real artery.

dimensional bending, building the 3D model we present in the next section.

4.3 Towards 3D patient specific model

In Figure 4.9 we show our first steps for the 3D patient specific model, as we said before, femoropopliteal artery bends and curves in every direction, so adding the third dimension to the model is absolutely mandatory in order to get the best solution.

We make some changes on the 2D model presented so far.

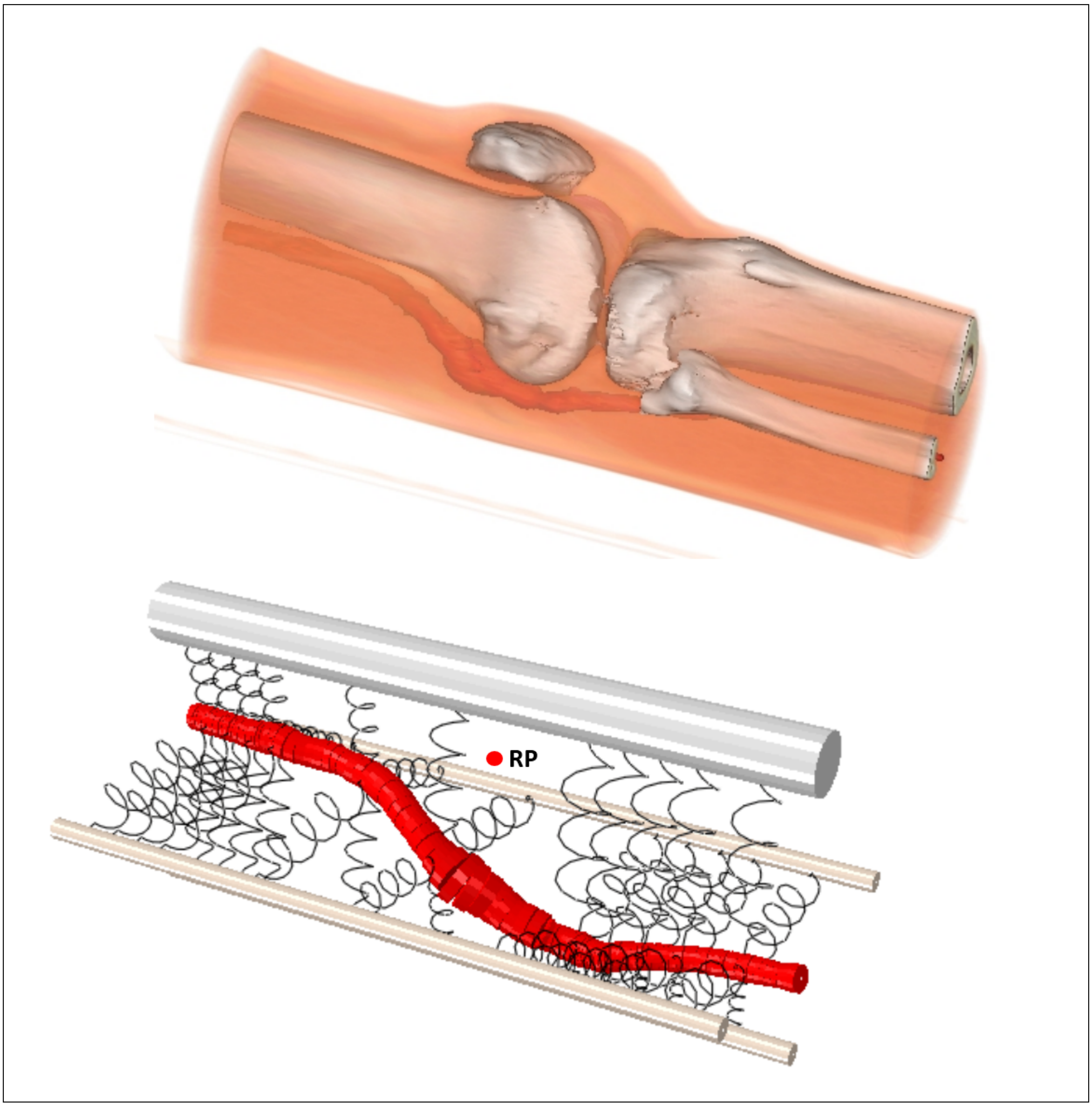

Figure 4.9: 3D patient specific model, at the top of the figure we show the volume rendering of the leg with the 3D model of bone and vessel, at the bottom our model with the patient's centerline and diameters and with the addition of lateral encasing.

We use the same patient's data, the one from Pisa.

In matlab scripts actually we don't modify so much the codes, we give the same parameters to

the code that calls functions to write the input file exactly as before, the difference is only the addition of the two new lateral parts of the encasing.
The main changes are in the Abaqus model itself, in fact now we have 9 three dimensional *BEAM* elements, the four more new lateral beams are still modeling the encasing of the leg, lateral limits of the thigh and the calf. Hence now we have *B31* elements, (DassaultSystèmes, 2014).
The artery part here has also the third component of the centerline's nodes coordinates, so we increase more the patient specificity at the beginning of the analysis.
All the properties of the new four beams are identical to the bone's properties and we use the same two materials of before.
Interaction are all unchanged and even boundary conditions, we just add the same boundary conditions of the other encasing parts to the new four. In particular we implement prestretch in the same way but shortening also the two new lateral thigh limits.
The type of *Spring element* and the stiffness setted are the same.
We still have the two *Static General* steps with large deformations involved, prestretch and flexion, and we run the *Full Analysis*.
the main new feature of this model is that the artery now can bend even out of plane, following better the anatomic real configuration of the vessel, in Figure 4.10 the first result is showed, lateral springs contain deformations along those directions exactly how tissues and muscles do in the real leg.

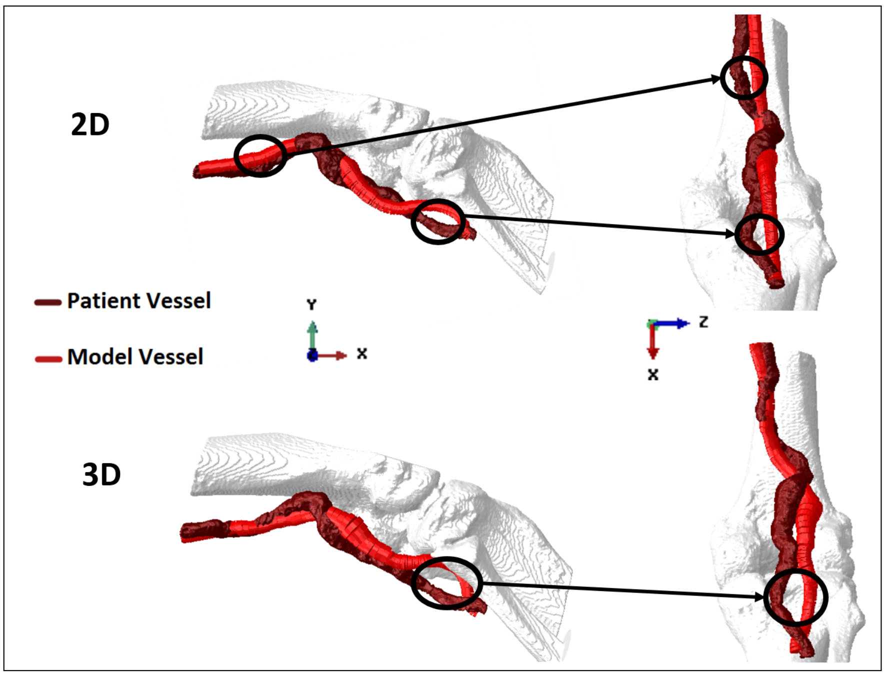

Figure 4.10: The artery part now is able to curve even along Z axis, but we still have the same error at the distal part of the vessel.

Obviously the model needs more work to fit on the real vessel with a low error, first of all we want to determine a solid relationship between springs' stiffness and tissues/muscles behavior, then we will evaluate if we should add some more patient specific boundary conditions, still related to the anatomy, for example adding a constraint where we have the adductor hiatus that can impose some particular deformation to the vessel.
Hence, once the model is optimized and follows the real anatomic artery deformation we will add the stent, maybe finding a better way even to model the device itself.
This should be the final step of all the project, even though it needs more work, this first results we get are very promising, even because also adding the third dimension and the resulting increasing of degree of freedom and variables, the computational cost does not grow (still lower than 10 seconds).
Working and improving this model we will try to reach the final goal to have a quick and simple but reliable tool of treatment's prediction for the complex biomechanics of the femoropopliteal artery.

Chapter 5

About internship at UNMC

During this project of thesis I spent one month, in April, at the University of Nebraska Medical Center in Omaha, Nebraska (USA) and I worked with Dr. Kamenskiy and Dr. Mac Taggart group of research in the surgery department of the center, in fact all of this work is in collaboration with this group, and it has been a great experience for many reasons.
I had the chance to work in a new environment, in an hospital, in close contact with surgeons and medical scientists; talking with them and attending their seminars and classes I learned a lot about peripheral arteries and veins, pathologies, old and new treatments, studies and new developments that are going on there.
The main reason of my visit was the cadavers' disection, in fact this group has the possibility to use light embalmed cadavers for their studies about kinematics and behavior of femoropopliteal artery, as we can see in MacTaggart et al. (2014) and Kamenskiy et al. (2016), this cadavers are from people who decide to donate their body for scientific purposes. The use of lightly embalmed cadavers as opposed to those that are fully embalmed, in their opinion, allows better preservation of natural tissue properties.
From the first of the two studies recalled here, we can have an idea of how they make kinematics measures, useful also for our model, they use, indeed, that string with laser-cut Nitinol markers placed on it.
Actually now the Nitinol devices are renewed, they aren't anymore the ones of the paper, but now they have four legs, instead of two, one is longer and thicker than the others so it can be recognize in the CT scans. It is worth noting that this devices don't deform the vessel, don't impose additional stresses and, for this reasons, they have a short range of axial movement given by the beads placed 2 cm apart that separate the devices one from the other.
With this markers they make measurements about deformations, i.e., axial compression, bending, torsion ad radial force, of the vessel during knee flexion with or without stents deployed in it, in appendix C we have an example of how this measures are calculated. At the end of kinematics

studies they extract the artery from the body and study it for histological classification and tissues' behavior.

When I was there we studied a cadaver of an old woman, 83 years old, with apparently no peripheral vascular diseases, the peripheral vessels were all patent. The cause of death was an aspiration pneumonia and coronary artery disease.

The procedure we followed is: at the beginning the surgeon, in particular Dr. Mac Taggart or Dr. Paulson, made a cut and the external iliac artery was exposed through a supra-inguinal retroperitoneal approach. Utilizing fluoroscopic guidance (GE-OEC Medical Systems Series 9800 Cardiovascular mobile digital C-arm system) a 80cm 9-French sheath (Cook Medical, Bloomington IN, USA) was canulated from the access site to the the tibioperoneal trunk over a .035" diameter wire (Boston Scientific, Natick MA, USA). Markers were then deployed 1–2 cm apart within the in situ iliac, femoral and popliteal arteries using a sheath. This method of intra-arterial marking allowed maintaining the integrity of the anatomical structures surrounding the FPA.

Arteries were pressurized, from a cut in the carotid, using a 37°C radiopaque custom mixture fluid and a pulsatile pump that allowed to avoid tissue swelling that can distort anatomical structures. Then, we got CT images (GE Light Speed VCTXT scanner GE Healthcare, Waukesha, USA) of limbs in the standing (180°), walking (110°), sitting (90°), and gardening (60°) postures were acquired with 0.625 mm axial resolution.

After the first set of images, we removed the markers from the vessels and we deployed in the left and right femoropopliteal artery stent devices, in particular in the right leg a 7X150mm Lifestent®, in the left leg a 6x100 Abbott Absolute pro® and a 7x100 Abbott Absolute pro® with an overlap of 1 cm, then we re-inserted the markers and we re-perfused the cadaver. After that we performed again CT scans for the same knee flexion angle.

This data we took will be crucial for our model, in fact we will validate it with the measures and deformations in different knee bending before the stent and we will try to predict the change in vessel behavior after a stent deploying, comparing our result with the real stented cadaver CT images.

When we finished with the CT scans, the next step was the disection of the leg to excise the artery from the body, in this moment we measured the length of the artery in-situ and the length of the artery excised (Kamenskiy et al., 2016). We found a longitudinal prestretch value (LPS) of 1.1, instead of 0.9 calculated from the equation of the paper that we use for our study, this woman had an LPS proper of a younger person. The excised artery will be used in the lab to evaluate other parameters.

This particular experience has been, for me, very useful, I think it is very important to understand how the human body actually is and works, I have now clear where the artery passes and goes, through which structures, muscles, tendons and tissues in general, and this is fundamental in order

to set the right boundary condition or modify the model in a more physiologic way, moreover I could see, touch and actually deploy different kind of stent devices.
Thank to my co-mentor Dr. Kamenskiy, who invited me to spend this month in his laboratory, I had this great possibility that I couldn't have otherwise for many reason; in fact the Nebraska law allow people to donate their body for scientific study, and here is prohibited, then working with cadavers is so expensive, the body itself costs so much and even all the devices: fluoroscopy, catheters, all of the different stents they use for the study and a CT Scan machine and they can afford all of this stuff just beacuse they got big founding from the state and moreover they work in an hospital with surgeons, so it's easier to find and use at least all of this machineries without the need to buy them.
Another interesting thing i learned during my stay, with the teaching of Eng. Paul Deegan technician of the laboratories in the surgery department, is to dissect arteries already excised from the body.
In the laboratories they are dissecting a large number of arteries and they are using them for many reasons, following always the same method that I learned step by step.
When the femoropopliteal artery arrived, in 0.9% NaCl physiological saline solution on ice, it needed to be disected because there were still some tissues, fat and the femoropopliteal vein attached to it; so the first step was to free the artery from all of this useless parts and clean it as in Figure 5.1.

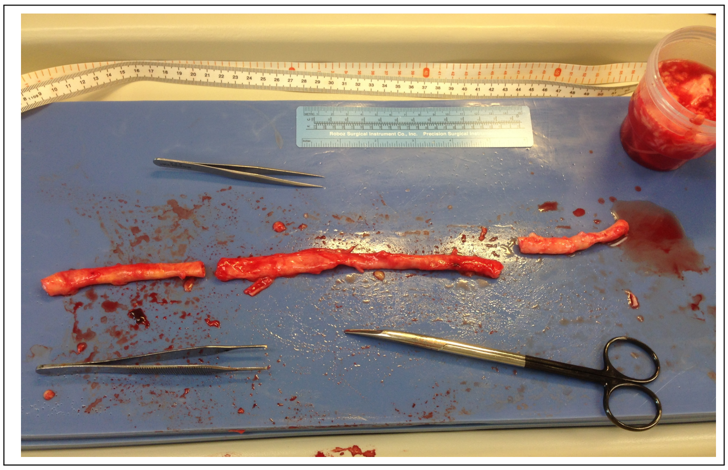

Figure 5.1: Femoropopliteal artery segment dissected by me during my period at UNMC in Omaha with the help of Eng. Paul Deegan.

Once the artery was clean first we measured the length and we compared it with the measures taken inside the body, for evaluating the longitudinal prestretch (in fact inside the vial containing the artery there was always a string of the same length of the artery in-situ).
Then we cut pieces of the artery, as little rings of approximately 2 mm in length, we photographed them and cut radially for a first histological evaluation of tissues at the microscope and to evaluate the axial prestretch (i.e, how much the artery opens after a radial cut).
After measuring the opening angle, index of axial prestretch, the entire arterial segment was cut longitudinally and spread out into a flat sheet, some square specimen from different part of the whole artery (diseased part or healthy part), were cut, preserving the in vivo longitudinal and circumferential orientations parallel with the specimen's square edges.
With these last specimens we performed biaxial tensile test attaching artery tissue to stainless steel hook. During testing, specimens were completely immersed in 0.9% NaCl physiological saline solution at 37°C. With an automatic software we registered the mechanical properties and behavior of each specimen in circumferential and longitudinal direction, Figure 5.2.

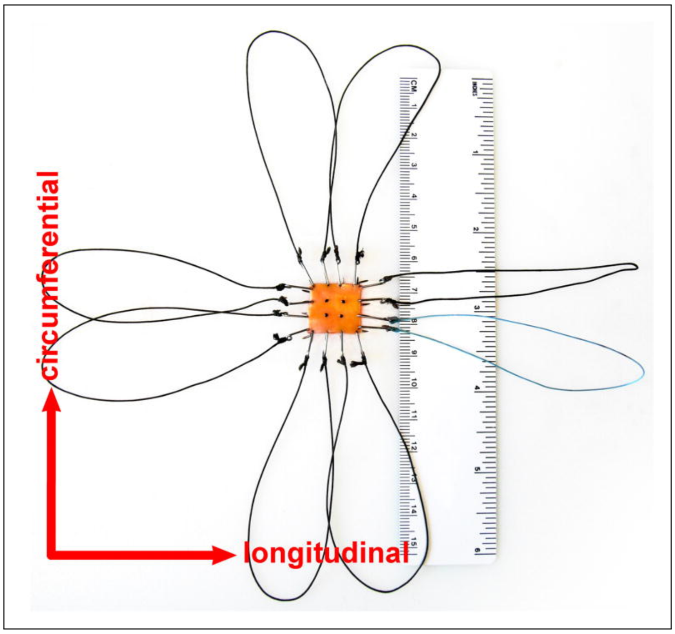

Figure 5.2: Specimen for biaxial testing (Kamenskiy et al., 2013)

After biaxial testing, all tissues were fixed in 10% neutral-buffered formalin, embedded in paraffin and sliced 5 μm thick to additional histological evaluation. All of this procedure is well described in Kamenskiy et al. (2013).
With this other new experience I could effectively touch the vessel's tissues and, moreover, I start to recognize pathologic artery from the healthy ones, I saw aneurysms, stenosis and atherosclerotic

plaques, very similar to pebbles, understanding why they can be so dangerous for Nitinol stent devices.

Dissecting, I deeply understood what is the difference between arteries and veins a between different tissues, tendons, vessel and fat.

These are the two main new experiences I have done in Nebraska, but I also helped Dr. Kamenskiy with an interesting literature review on all the computational models existing, about mechanics and fluid dynamics, that I reported in the first chapter.

I worked a lot with a Dr. Kamenskiy's master student for solving some issues about a CAD stent model they want to create in order to perform some simulation on a specific design. I also processed some data taken from older cadavers' dissection, useful for a code that Dr. Anstasia Desyatova wrote to evaluate stent solicitation from displacement field of the vessel (coming from knee flexion at different angles).

Chapter 6

Conclusions and future work

The aim of the present study is to develop a simple simulation-based model of FPA able to reproduce the main biomechanical features of this arterial region. For this purpose, we have first performed a literature review about this topic. Such a survey shows the open issues existing in literature about femoropopliteal artery and his kinematics. In this region the incidence of pathologies is increasing and a well functioning, reliable, mini-invasive treatment does not exist yet. The main problems are therefore to understand the deformation of the vessel due to knee flexion and to define correct design and material for an endovascular device, such as a stent, that can be durable if deployed in this artery. In literature we have many studies about deformation of the vessel that gave us ideas on what was important to evaluate in our project and we find also many numeric model able to simulate the behavior of this region. The overview of the computational model highlights that the biomechanical analysis of femoropopliteal artery needs to be improved for finding novel solutions with a lower computational cost.
Given the available studies, we have developed a computational model based on structural finite element analysis. The model is composed mainly by beam and spring elements allowing fast simulation even on a standard laptop.
In fact we evaluated the behavior of the artery with ageing and with a stiffer portion in it, simulating a stent, and we found that this simple assembly of beam and spring can give the result we expected, curvature and tortuosity increase with age but decrease within the stent, causing kinks in other parts of the artery. The main limitation of this model is the lack of patient specificity so the further improvement see the addition of patient data to the model. We created a second model adding some information to the parts such as the centerline of the real patient's artery extracted from medical imaging and real values of diameters, also the age of the patient now is a known parameter, to put in relation with the prestretch. Overlapping the result of the FE analysis and the 3D model, reconstructed from CT scan of the patient, the result is very interesting, keeping the computational cost definitely low. Besides of a problem regarding the implementation of the

prestretch that is still to be solved, the other principal issue was the hypothesis to limit the model in a 2D environment. For this reason we are moving to the 3D patient specific model and the preliminary results we got from the simulation are promising.
At the end of this work I describe the internship at the UNMC in Omaha (USA), outstanding experience that gave me the possibility to be present at experiment on cadaver and dissection of femoropopliteal artery, from which I got data that will be useful in the future to validate our models.
In the future works we consider to improve patient specific models, especially the 3D one. We would like to find a relationship between spring's stiffness and surrounding tissue's stiffness, maybe we will add some additional boundary condition in places where we know there are anatomical constraints, an example is the adductor hiatus where the artery pass through to go in the popliteal fossa that can induce particular deformations and bending. After we will have refined the model, the final aim is to validate it respect patient specific data extracted by in-vivo images or ex-vivo experiments to predict the impact of stenting.

Appendix A

Format input file

The explanation here below is taken from DassaultSystèmes (2010).
The *input file* is the means of communication between the preprocessor, usually Abaqus/CAE, and the analysis product, Abaqus/Standard or Abaqus/Explicit. It contains a complete description of the numerical model.
The input file is a text file that has an intuitive, keyword based format, so it is easy to modify using a text editor if necessary; if a preprocessor such as Abaqus/CAE is used, modifications should be made using it.
The example of an overhead hoist, shown in Figure A1, is used to illustrate the basic format of the Abaqus input file, The hoist is a simple, pin jointed truss model that is constrained at the lefthand end and mounted on rollers at the righthand end. The members can rotate freely at the joints. The frame is prevented from moving out of plane. A simulation is performed to determine the structure's deflection and the peak stress in its members when a 10 kN load is applied as shown in figure.

In the Figure A2 below we present the input fil format related to the figure of the hoist.
It is divided in two parts; the first section contains *Model Data* and includes all the information required to define the structure being analyzed. The second section contains *History Data* that define what happens to the model: the sequence of loading or events for which the response of the structure is required.

The input file is composed of a number of option blocks that contain data describing a part of the model.
Each option block begins with a *keyword line*, which is usually followed by one or more *data lines*. These lines cannot exceed 256 characters.

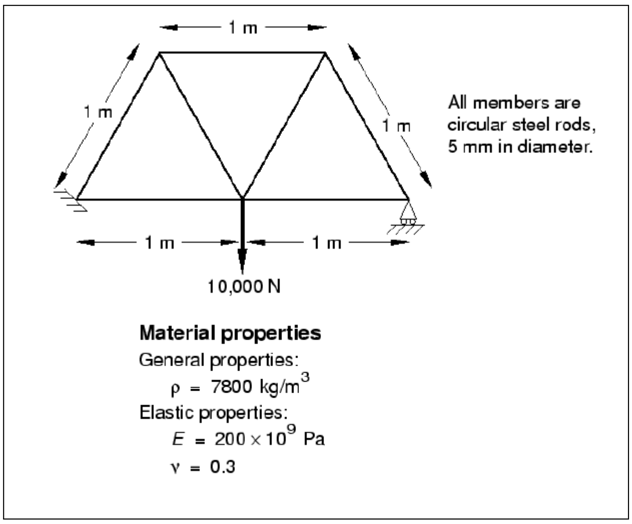

Figure A1: Schematic of an overhead hoist (DassaultSystèmes, 2010)

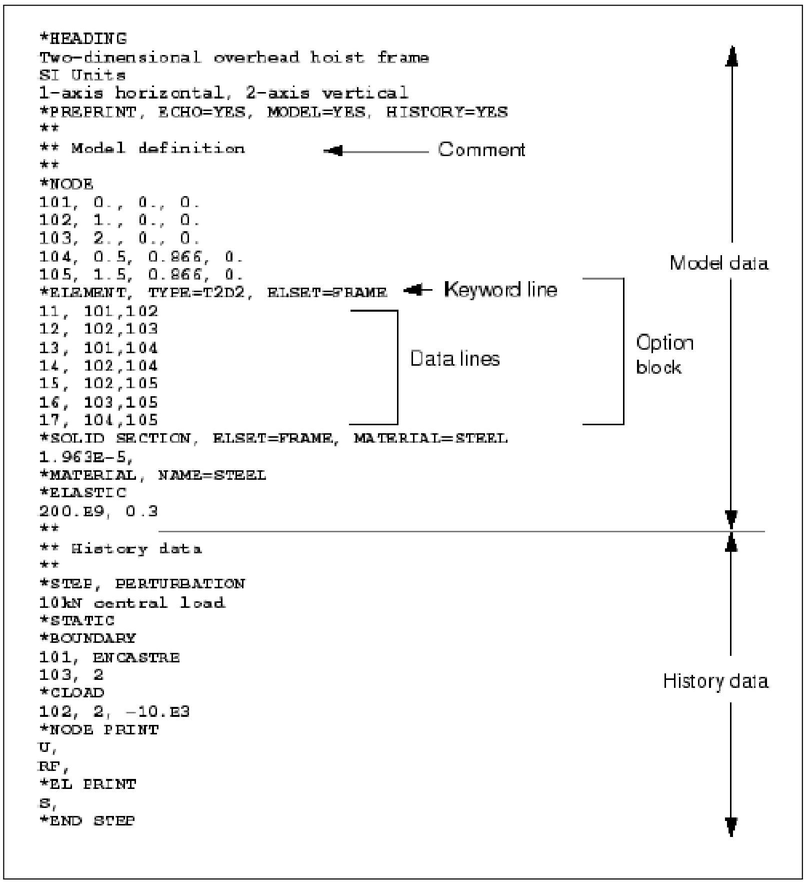

```
*HEADING
Two-dimensional overhead hoist frame
SI Units
1-axis horizontal, 2-axis vertical
*PREPRINT, ECHO=YES, MODEL=YES, HISTORY=YES
**
** Model definition
**
*NODE
101, 0., 0., 0.
102, 1., 0., 0.
103, 2., 0., 0.
104, 0.5, 0.866, 0.
105, 1.5, 0.866, 0.
*ELEMENT, TYPE=T2D2, ELSET=FRAME
11, 101,102
12, 102,103
13, 101,104
14, 102,104
15, 102,105
16, 103,105
17, 104,105
*SOLID SECTION, ELSET=FRAME, MATERIAL=STEEL
1.963E-5,
*MATERIAL, NAME=STEEL
*ELASTIC
200.E9, 0.3
**
** History data
**
*STEP, PERTURBATION
10kN central load
*STATIC
*BOUNDARY
101, ENCASTRE
103, 2
*CLOAD
102, 2, -10.E3
*NODE PRINT
U,
RF,
*EL PRINT
S,
*END STEP
```


Figure A2: Format of Abaqus input file (DassaultSystèmes, 2010)

Appendix B

Previous model

Before the models we present in this thesis project, we made a lot of attempts in order to find a well-functioning solution. Here below we briefly show how was the first model we implemented and then a simpler "toy" model we created, in order to understand how to make it all works, and finally a matlab script I wrote for calibrating springs and helping to reach the real artery's configuration. All this steps are summarize in workflow in Figure B1.

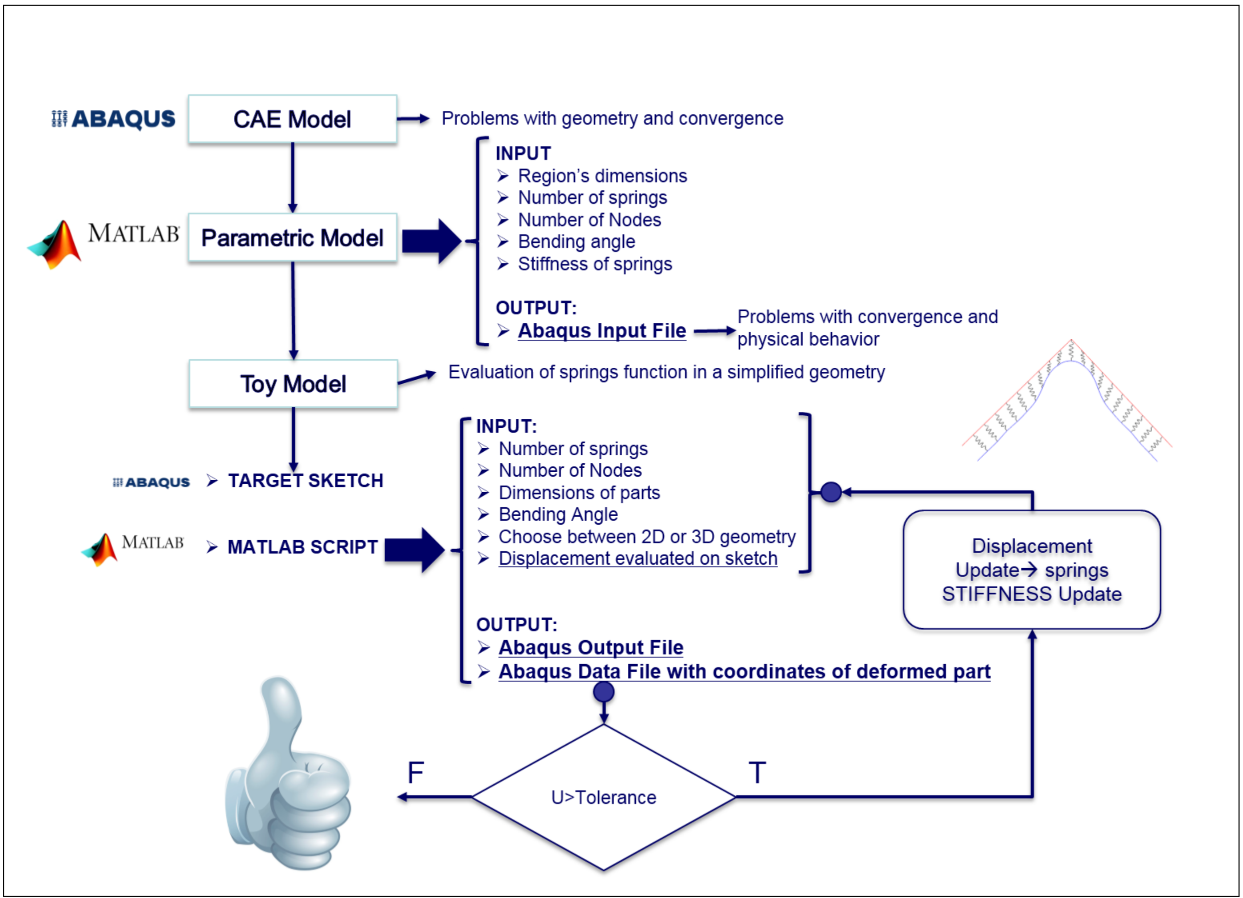

Figure B1: Workflow of the first part of this work, containing all the attempts we made to get to our solution. We tried to reach convergence even with a CAE model and with a parametric script. Then we implement the *Toy Model* with a simplified geometry. Once we reach convergence we performed calibration of springs based on the error between a target sketch and our deformed part, this error had to be within a certain tolerance.

B.1 Our first model

Here below in Figure B2 we decribe what was the structure of the first model we made, as anatomic reference we use the CT images of the cadaver received from Dr. Kamenskiy.

For creating this model we used a Matlab script similar to the others already described, we used

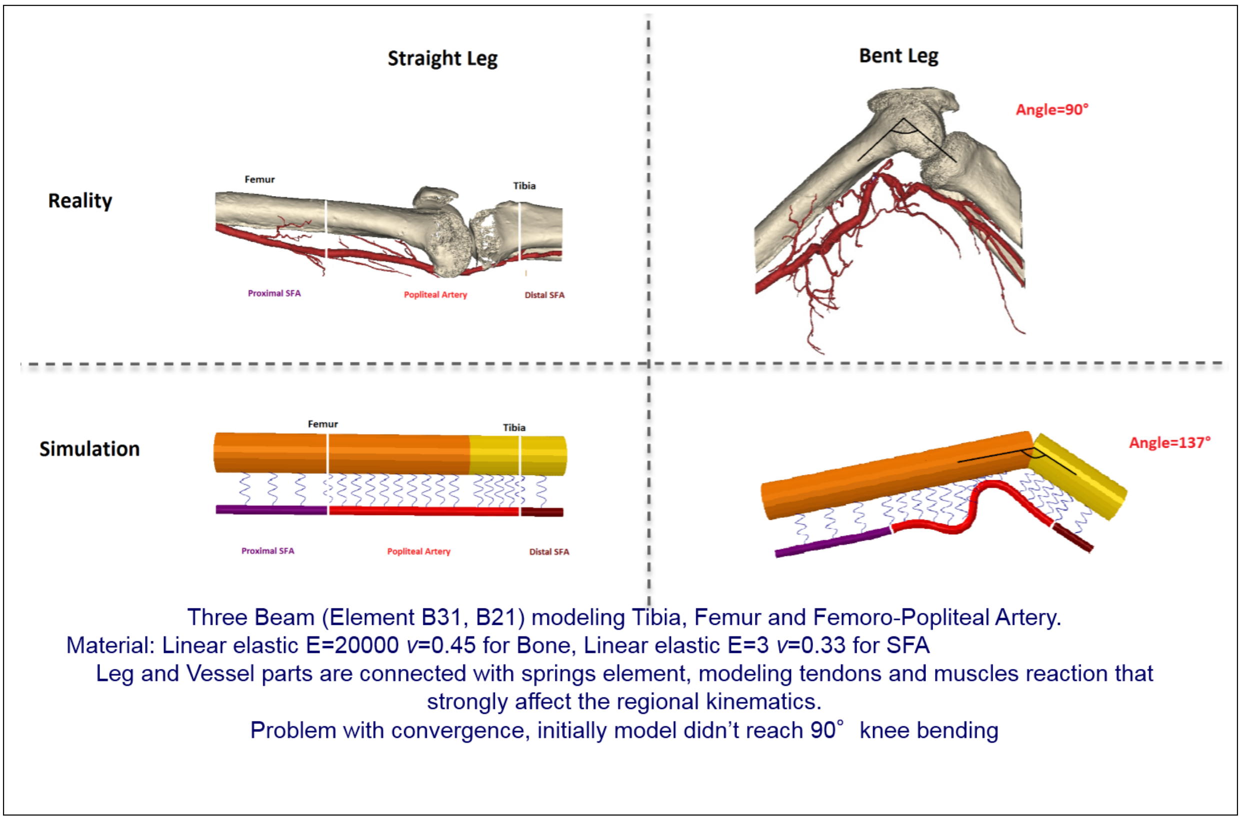

Figure B2: Schematic of the first model. At the top we have the 3D reconstruction of the CT scan in straight and bent leg configuration. At the bottom the model with (on the right) the result of te simulation; as we can see we couldn't reach the 90° knee bending.

beam elements, but three in this case; one for the FPA, one for the femur and one for the tibia. Here the rotation center is the last node of the femur and the tibia should rotate around it. Spring are still *SpringA* element.

Unfortunately this model didn't reach convergence, although we made several various attempts.

For this reason we decided to simplify the model, using a symmetric general geometry to understand better the function of the springs, behavior of the beam and interaction between them.

B.2 Toy model

This model had a simplified simmetric geometry, still with beams elements and springs, in the Figure B3 below we can see the sketch of the toy model and the result of the simulation.

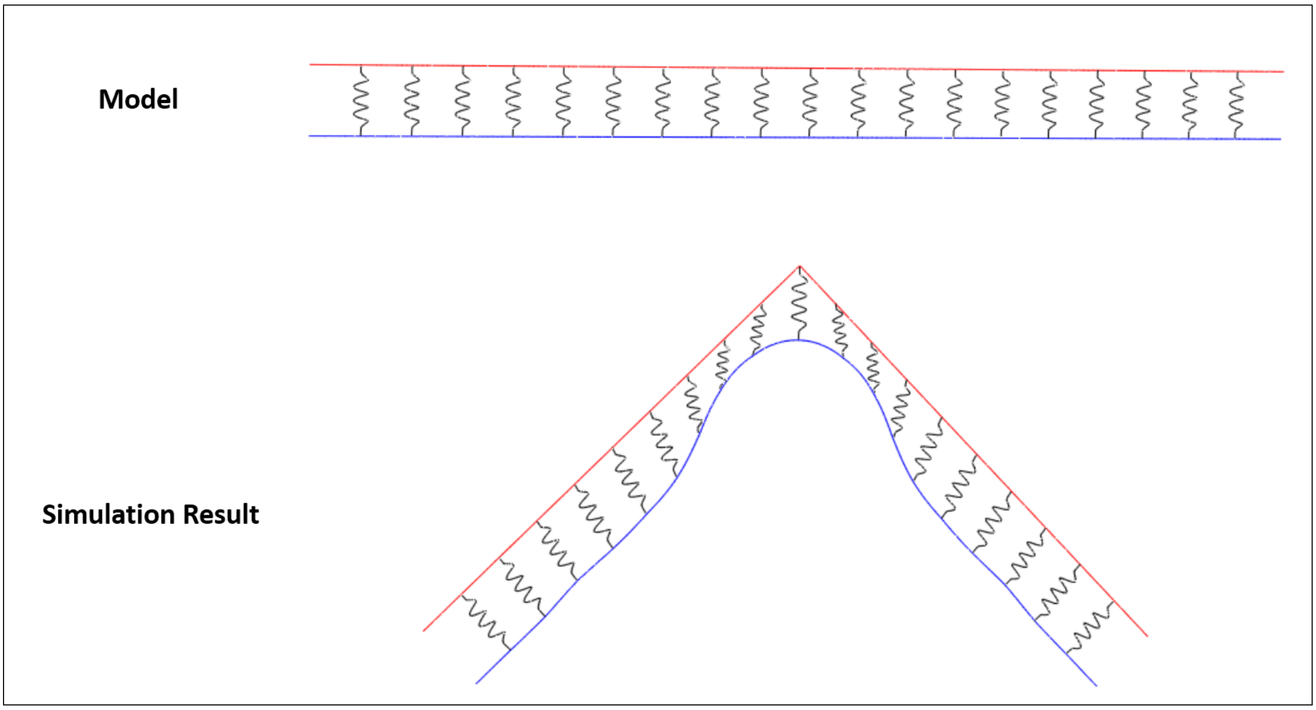

Figure B3: At the top of the image we have the sketch of the model at the bottom the result of the simulation.

B.3 Spring calibration

Once we made the toy model reach the convergence we wrote a script to implement springs calibration.

The script extracts, from the output .DAT file, the coordinates of the requested part in the last time step of the analysis. It extracts the nodes where the springs are attached. Then compare these nodes with the ones of the target sketch; if the distance 'U' between the two nodes is over a determined tolerance we increase or decrease (depending on the error, if it is positive or negative) the spring's stiffness in that node.

Even though all seemed working, and in Figure B4 we show some preliminary results, actually we understood here that springs are not so sensitive to the displacements as we thought, so reaching the tolerance for all the nodes at the same time was impossible.

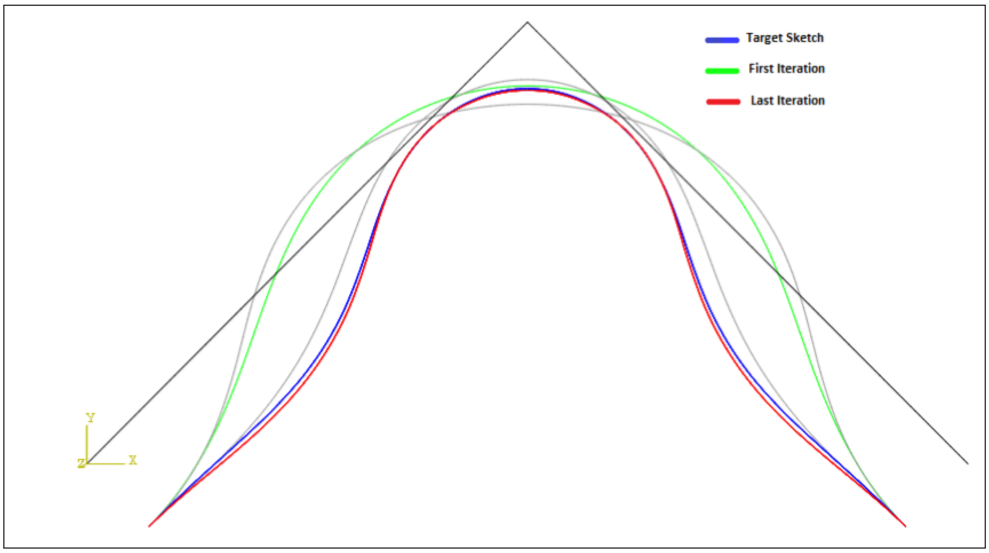

Figure B4: Preliminary result of spring's calibration.

Appendix C

FPA deformation measurements

With the help of Dr. Kamenskiy, we made some measurements on Mimics (MaterializeCo.,Leuven,Belgium) on the cadaver's CT images received, as the group of Omaha normally does after every cadaver's dissection. Actually we measured axial compression, bending, torsion, radial force using markers and the Dr. Kamenskiy's method, (MacTaggart et al., 2014), then we used two different ways to calculate curvature, with Mimics tool and with VMTK comparing the two results.

C.1 Marker measurements

C.1.1 Axial compression

We used Mimics *Distance over centerline* tool for measuring distance between two consecutive markers in bent 'li' e straight 'Li' configuration. Here below the equation used to calculate axial compression, in Figure C1 we show the values.

$$Li/li = \frac{Distance\_bent}{Distance\_straight} \tag{C.1}$$

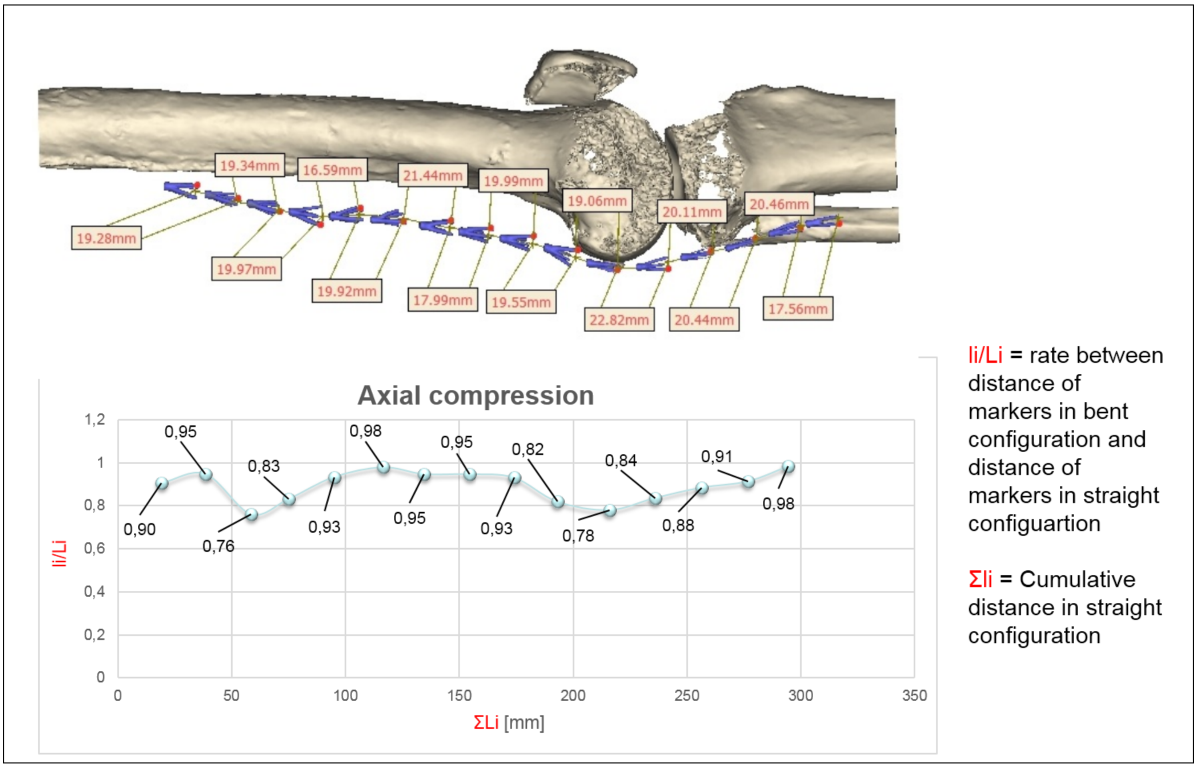

Figure C1: Values of axial compression found.

C.1.2 Bending

Inscribing sphere into curvature of centerline.

$$Curvature = \frac{1}{R} \tag{C.2}$$

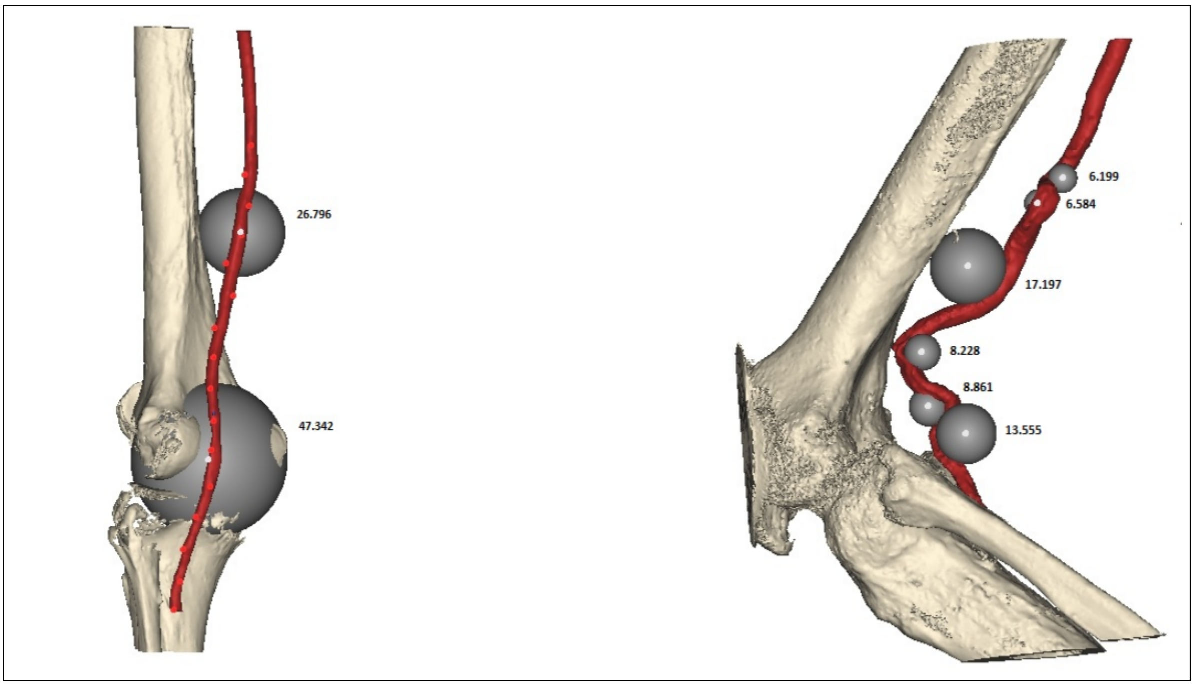

Figure C2: Values of bending found.

C.1.3 Torsion

Angle of rotation (counterclockwise) between two consecutive markers in bent and straight configuration.

$$\Delta_i = \textit{bent angle–straight angle} \tag{C.3}$$

If $|\Delta_i| > 180$, then calculate torsion angle as:

$$(|\Delta_i| - 360) \cdot \frac{\Delta_i}{|\Delta_i|} \tag{C.4}$$

Rotation per unit of straight artery length:

$$t_i = \frac{\Delta_i}{L_i} \tag{C.5}$$

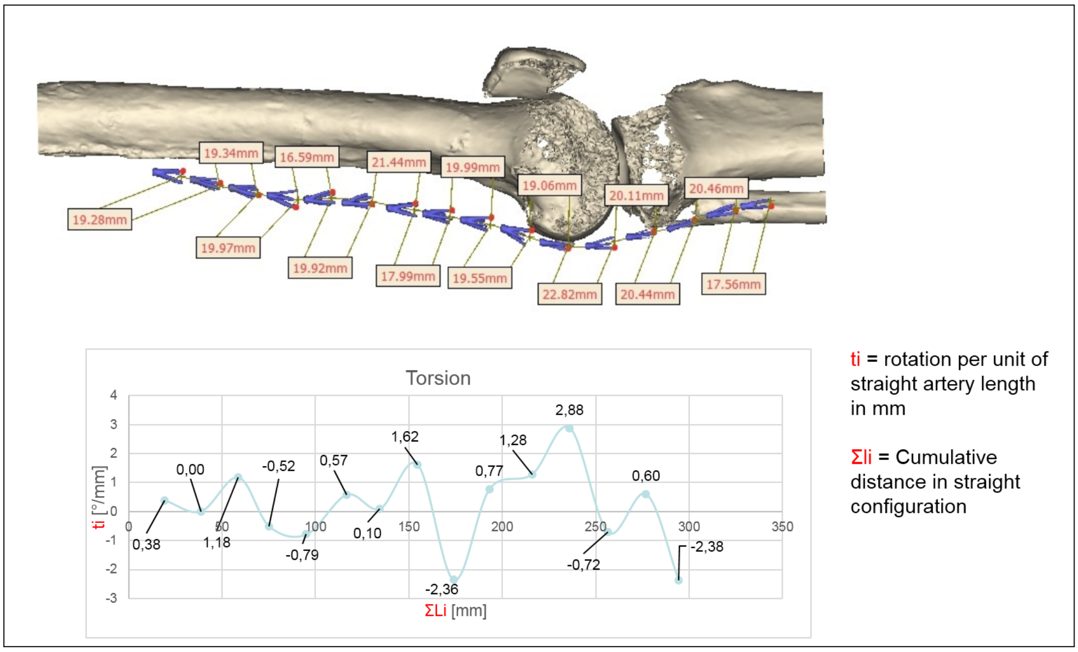

Figure C3: Value of torsion found.

C.1.4 Radial compression

Evaluate as the distances between the two longest legs of each device on the straight and bent configuration.
Difference between the initial opening of the device and the current opening.

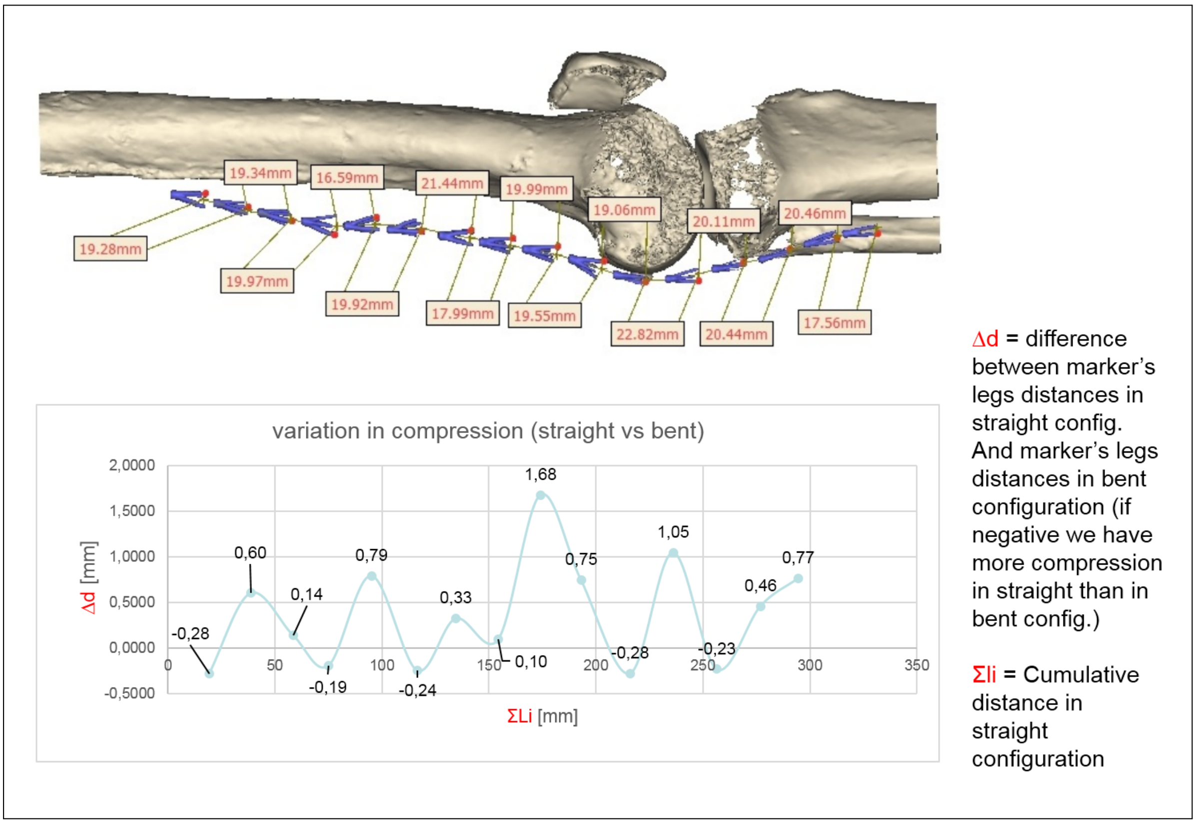

Figure C4: Values of radial compression found.

C.2 Curvature comparison

Besides the "sphere method" proposed by Dr. Kamenskiy we decided to measure curvature in two more different ways and compare the results; the first with *Centerline Curvature* tool in Mimics and in the second we calculated the centerline of the vessel with *vmtkcenterlines* tool of VMTK and then we evaluate curvature with the other VMTK script *vmtkcenterlinegeometry*. Result of comparison in Figure C5 for the straight leg and Figure C6 for the bent leg.

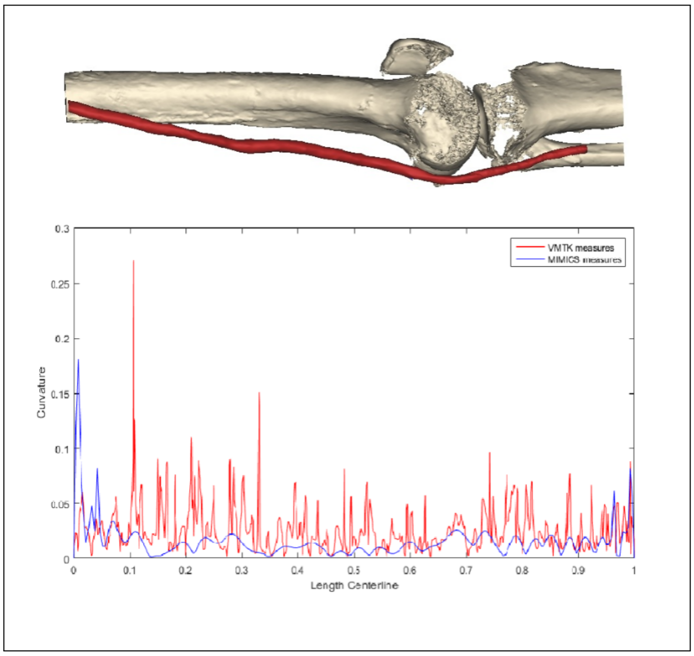

Figure C5: Curvature comparison in straight leg.

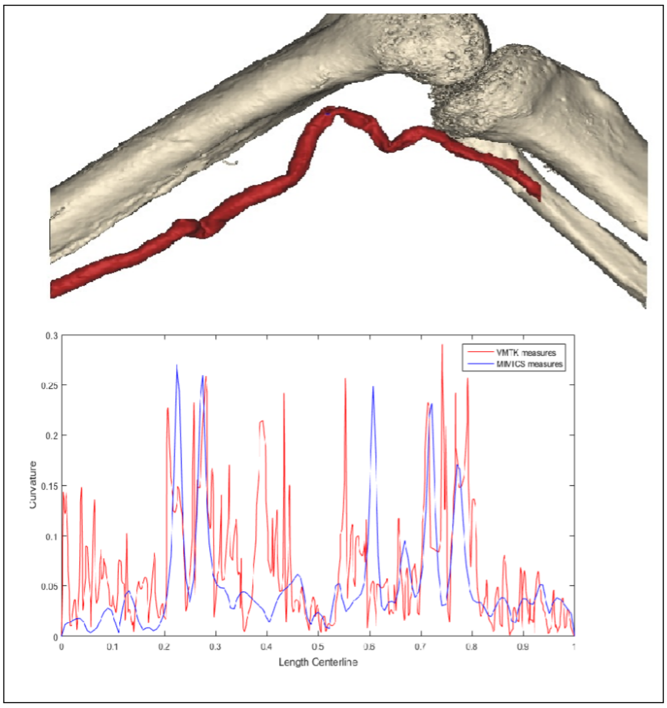

Figure C6: Curvature comparison in bent leg.

Appendix D

Table of Abbreviations

Here below are reported in alphabetical order all the abbreviation used in the work:

Abbreviation	**Significate**
3D	Three Dimensional
2D	Two Dimensional
CAE	Computer Aided Engineering
CAD	Computer Aided Drafting
CT	Computed Tomography
DICOM	Digital Imaging and COmmunications in Medicine
FEA	Finite Element Analysis
INP	INPut format
MRI	Magnetic Resonance Imaging
NITINOL	NIckel TItanium Naval Ordinance Laboratory
STL	Surface Tessellation Language
VMTK	Vascular Modelling ToolKit
FPA	FemoroPopliteal Artery
SFA	Superficial Femoral Artery
LPS	Longitudinal PreStretch

Bibliography

Alexander Nikanorov, B. S. (2009). Fracture of self-expanding nitinol stents stressed fracture of self-expanding nitinol stents stressed in vitro under simulated intravascular conditions.

Cheng, C., G. Choi, R. Herfkens, and C. Taylor (2010). The effect of aging on deformations of the superficial femoral artery resulting from hip and knee flexion: Potential clinical implications. *Journal of vascular and interventional radiology 21*(2), 195 – 202.

Cheng, C. P., N. M. Wilson, R. L. Hallett, R. J. Herfkens, and C. A. Taylor (2006). In vivo {MR} angiographic quantification of axial and twisting deformations of the superficial femoral artery resulting from maximum hip and knee flexion. *Journal of Vascular and Interventional Radiology 17*(6), 979 – 987.

Choi, G., C. Cheng, N. Wilson, and C. Taylor (2009). Methods for quantifying three-dimensional deformation of arteries due to pulsatile and nonpulsatile forces: Implications for the design of stents and stent grafts. *Annals of Biomedical Engineering 37*(1), 14–33.

Collaboration, A. B. I. (2008). Ankle brachial index combined with framingham risk score to predict cardiovascular events and mortality: A meta-analysis. *JAMA 300*, 197–208.

Conti, M., M. Marconi, G. Campanile, A. Reali, D. Adami, R. Berchiolli, and F. Auricchio (2016). Patient-specific finite element analysis of popliteal stenting. *Meccanica*.

DassaultSystèmes, . (2010). Abaqus 6.10, getting started with abaqus, keyword edition. http://abaqusdoc.ucalgary.ca/pdf_books/GET_STARTED_K.pdf.

DassaultSystèmes, . (2014). Abaqus student edition 6.14 documentation. http://127.0.0.1:2080/v6.14/books/usb/default.htm.

Diehm, N., S. Sin, H. Hoppe, I. Baumgartner, and P. Büchler (2011). Computational biomechanics to simulate the femoropopliteal intersection during knee flexion: A preliminary study. *Journal of Endovascular Therapy 18*, 388 – 396.

Ganguly, A., J. Simons, A. Schneider, B. Keck, N. R. Bennett, and R. Fahrig (2011). In-vitro imaging of femoral artery nitinol stents for deformation analysis. *Journal of Vascular and Interventional Radiology 22*(2), 236 – 243.

Ghriallais, R. and M. Bruzzi (2013). Effects of knee flexion on the femoropopliteal artery: A computational study. *Medical Engineering* & *Physics 35*(11), 1620 – 1628.

Ghriallais, R. and M. Bruzzi (2014). A computational analysis of the deformation of the femoropopliteal artery with stenting. *Journal of Biomechanical Engineering 136*, 071003–071003–10.

Giordana, S., S. J. Sherwin, J. Peiro, D. J. Doorly, J. S. Crane, K. Lee, N. J. W. Cheshire, and C. G. Caro (2005). Local and global geometric influence on steady flow in distal anastomoses of peripheral by-pass grafts. *Journal of Biomechanical Engineering 127*, 1412–1418.

Hernando, F. J. S. and A. M. Conejero (2007). Peripheral artery disease: Pathophysiology, diagnosis, and treatment. *Revista Española de Cardiología*, 969–982.

Hurks, R., R. H. Kropman, C. W. Pennekamp, I. E. Hoefer, J. P. de Vries, G. Pasterkamp, A. Vink, and F. L. Moll (2014). Popliteal artery aneurysms differ from abdominal aortic aneurysms in cellular topography and inflammatory markers. *Journal of Vascular Surgery 60*, 1514–1519.

Kamenskiy, A., I. I. Pipinos, Y. A. Dzenis, C. S. Lomneth, S. A. J. Kazmi, N. Y. Phillips, and J. N. MacTaggart (2013). Passive biaxial mechanical properties and in vivo axial pre-stretch of the diseased human femoropopliteal and tibial arteries. *Acta Biomaterialia 10*, 1301 – 1313.

Kamenskiy, A., A. Seas, G. Bowen, P. Deegan, A. Desyatova, N. Bohlim, W. Poulson, and J. MacTaggart (2016). In situ longitudinal pre-stretch in the human femoropopliteal artery. *Acta Biomaterialia 32*, 231 – 237.

Kim, Y.-H., J.-E. Kim, Y. Ito, A. M. Shih, B. Brott, and A. Anayiotos (2008). Hemodynamic analysis of a compliant femoral artery bifurcation model using a fluid structure interaction framework. *Annals of Biomedical Engineering 36*, 1753 – 1763.

Liu, Y., Y. Lai, A. Nagaraj, B. Kane, A. Hamilton, R. Greene, D. McPherson, and K. Chandran (2001). Pulsatile flow simulation in arterial vascular segments with intravascular ultrasound images. *Medical Engineering* & *Physics 23*, 583 – 595.

MacTaggart, J. N., N. Y. Phillips, C. S. Lomneth, I. I. Pipinos, R. Bowen, B. T. Baxter, J. Johannin, G. M. Longo, A. S. Desyatova, M. J. Moulton, Y. A. Dzenis, and A. V. Kamenskiy (2014). Three-dimensional bending, torsion and axial compression of the femoropopliteal artery during limb flexion. *Journal of Biomechanics 47*, 2249 – 2256.

McGah, P. M., D. F. Leotta, K. W. Beach, J. J. Riley, and A. Aliseda (2011). A longitudinal study of remodeling in a revised peripheral artery bypass graft using 3d ultrasound imaging and computational hemodynamics. *Journal of Biomechanical Engineering*.

Mills, J. L. (2016). Infrainguinal disease: Surgical treatment. *Eighth Edi. Elsevier Inc.*.

Moayeri, M. S. and G. R. Zendehbudi (2003). Effects of elastic property of the wall on flow characteristics through arterial stenosis. *Journal of Biomechanics 36*, 525–535.

National Insitute of Health, N. (2015). What is peripheral artery disease? https://www.nhlbi.nih.gov/health/health-topics/topics/pad.

Norgren, L., W. Hiatt, J. Dormandy, M. Nehler, K. Harris, and F. Fowkes (2007). Inter-society consensus for the management of peripheral arterial disease (tasc ii). *Journal of Vascular Surgery 45*, S5–S67.

O'Brien, T. P., P. Grace, M. Walsh, P. Burke, and T. McGloughlin (2015). Computational investigations of a new prosthetic femoral-popliteal bypass graft design. *JOURNAL OF VASCULAR SURGERY*.

Ouriel, K. (2001). Peripheral arterial disease. *THE LANCET 358*, 1257–64.

Petrini, L., A. Trotta, E. Dordoni, F. Migliavacca, G. Dubini, P. V. Lawford, J. N. Gosai, D. M. Ryan, D. Testi, and G. Pennati (2015). A computational approach for the prediction of fatigue behaviour in peripheral stents: Application to a clinical case. *Annals of Biomedical Engineering 44*, 536 – 547.

Pressley, A. (2010). *Elementary Differential Geometry.* London.

Rivera, J., G. van der Graaf, J. Escudero, S. Bellmunt, and F. van de Vosse (2014). A cfd study on hemodynamics for different locations of the distal anastomosis of a bypass nearby a collateral vessel in the femoropopliteal area. *International Journal for Numerical Methods in Biomedical Engineering*, 1263–1277.

Schmidt, D., L. M. Asmis, B. Odermatt, J. Kelm, C. Breymann, M. Gössi, M. Genoni, G. Zund, and S. P. Hoerstrup (2006). Engineered living blood vessels: functional endothelia generated from human umbilical cord-derived progenitors. *The Annals of Thoracic Surgery 82*, 1465 – 1471.

Schuenke, M., E. Schulte, U. Schumacher, L. M. Ross, E. D. Lamperti, and M. Voll (2010). *Atlas of Anatomy, General Anatomy and Musculoskeletal System.*

Smouse, H., A. Nikanorov, and D. LaFlash (2005). Biomechanical Forces in the Femoropopliteal Arterial Segment What happens during extremity movement and what is the effect on stenting? *Endovascular Today*, 60–66.

Wensing, P., F. Scholten, P. Buijs, M. Hartkamp, W. Mali, and B. Hillen (1995). Arterial tortuosity in the femoropopliteal region during knee flexion: a magnetic resonance angiographic study. *Journal of Anatomy 187*(1), 133–139.

Wood, N. B., S. Z. Zhao, A. Zambanini, M. Jackson, W. Gedroyc, S. A. Thom, A. D. Hughes, and X. Y. Xu (2006). Curvature and tortuosity of the superficial femoral artery: a possible risk factor for peripheral arterial disease. *Journal of Applied Physiology 101*, 1412–1418.

Young, M., M. Streicher, R. Beck, A. van den Bogert, A. Tajaddini, and B. Davis (2012). Simulation of lower limb axial arterial length change during locomotion. *Journal of Biomechanics 45*(8), 1485–1490.

Yushkevich, P., J. Piven, H. Hazlett, R. Smith, S. Ho, J. Gee, and G. Gerig (2006). User-guided 3D active contour segmentation of anatomical structures: significantly improved efficiency and reliability. *NeuroImage 31*, 1116–1128.